
UNIVERSITA' POLITECNICA DELLE MARCHE

FACOLTA' DI INGEGNERIA

*Department of Information Engineering*

*Master's Degree in Biomedical Engineering*

# EXPERIMENTAL EVALUATION OF A WRIST-WORN DEVICE FOR THE MEASUREMENT OF THE GALVANIC SKIN RESPONSE

Supervisor:

**Prof. Susanna Spinsante**

Co-Supervisor:

**Prof. Stefania Cecchi**

Author:

**Agnese Piersanti**

A. Y. 2018-2019

# Contents

# Abstract

Electrodermal activity (EDA) is a property of the human body affected by changes in the skin resistance due to the effects of the sympathetic nervous system (SNS) on sweat glands permeability. Changes in EDA reflect the physiological processes related to emotions, that occur out of human control. In the last decades this biometric signal is gaining interest in the field of Emotion Recognition and for a variety of healthcare applications. One of the main objectives of the research carried out in this field is the development of classification algorithms able to recognize different emotions and to understand which is the kind of stimuli that evoked such response. However, the intra-individual variability of the EDA signal among different subjects makes the achievement of this goal still challenging. To increase the accuracy of classification systems for emotion recognition based on EDA signals, the scientific research is analysing which are the features with the highest information content for this particular signal. In this Thesis, 16 features have been extracted, 8 in the time domain and 8 in the frequency domain, and analysed in order to evaluate which of them has the highest significance and within what terms. The Empatica E4 wearable sensor was used for data acquisition in concomitance with a prototype static sensor, the Arduino UNO based GSR-Grove sensor to obtain simultaneous recordings and to evaluate the E4 sensor against the GSR-Grove one. The experiment focused on the ability of these sensors to predict relative physical activity intensity. The 4 enrolled subjects were asked to perform activities with 3 different levels of intensity: resting, medium and high intensity exercise. The obtained dataset consisted of 36 recordings for each sensor. Data were processed and analysed in MATLAB. What emerges from the results is that features' significance cannot be generalised for all the subjects and it is strictly dependent on intra-individual characteristics. There are features that result to be non-significant at all, but this should be confirmed by involving a larger population. Enlarging the study to a greater number of subjects could be promising in order to identify common EDA patterns for subclasses of subjects. This way it would be possible to design subject-dependent classification algorithms. Focusing on the two involved sensors, the Empatica E4 sensor resulted to be more reliable. This is an encouraging outcome for the future of EDA processing within the field of wearables.

# Chapter 1

# Introduction

Since the last decades of the 19th century, when human electroencephalogram (EEG) was yet an unknown recording, changes in the electrical activity of the skin were observed to occur in concomitance with psychological phenomena and were considered the origin of psychophysiological recordings. The variations of the electrical properties of the skin caused by sweat secretion can be measured in an easy and non-invasive way, applying a low constant voltage on the skin surface with the help of two electrodes. The so-obtained signal is referred to as Galvanic Skin Response (GSR), also known as Skin Conductance (SC) or Electrodermal Activity (EDA) [1]. GSR signals have been shown to be directly related to both positive and negative emotional arousal and excitement in response to stimuli. Moreover, the sweat glands innervation is exclusively under the control of the sympathetic nervous system (SNS) and this strict relationship contributes to make GSR an interesting signal for many fields of application. Sweat secretion is an autoregulatory process which is not under conscious control, because it is regulated by the SNS, that is part of the autonomic nervous system. In daily circumstances such as fear, anxiety, stress, joy or under physical exercise, our body starts to sweat, even if sometimes imperceptibly. Hence, the GSR can be exploited to measure sympathetic activity and, consequently, to have a feedback of those hidden mechanisms that occur out of our control [2]. GRS signal is gaining much interest because it could be exploited in a variety of applications that are nowadays involved in different fields. In psychological research, aspects related to personal experience and personality of the subject could be obtained and used for therapy. Moreover, many researchers consider the GSR signal a good indicator of stress levels to help early detection of a chronic stress condition, which could lead to cardiovascular and gastrointestinal diseases, anxiety disorder and depression. With the emergence of wearable devices capable to provide biometric information to the users, the possibility of stress self-management is becoming a true reality [3]. In case of psychiatric disorders such as schizophrenia, depression, post-traumatic stress disorder, autistic spectrum disorders, addiction, eating disorders, GSR signals could be used as biofeedback by giving a quantitative measure of the

hyperarousal and supporting the evaluation of both the efficacy of the therapy and the severity of illness. Other examples of clinical applications are cases of pain assessment or peripheral neuropathies [4]. In the sport field, measuring GSR in different training sessions, or before and after a positive or negative performance, could be useful to evaluate the best training schedule for athletes [5]. Marketing research could greatly benefit from GSR signal processing, to evaluate consumer preferences, the impact of contents and products and understand people engagement in advertising, media, videogames, social networks and films [6]. Software usability testing is another application in which the GSR signal could be used, to evaluate and improve the usability of software and websites, to keep user stress level and confusion as low as possible [7]. GSR combined with other physiological measures, such as heart rate and respiration, can also determine if a person is telling the truth or not [5]. This roundup of applications has been reported in order to highlight the great potential of the EDA signal and the high number of research fields in which its study is spreading. All these applications have in common the need to quantify and identify the type of stimulus to which the galvanic response is associated. To achieve this goal, recent studies are trying to use classification algorithms. Emotion recognition with the use of classifiers has been explored in the literature in the last years employing the computation of different features [8]. However, GSR signal has a great variability due to the different contexts in which the signal could be acquired and to physiological variability among the individual subjects. This variability makes it difficult to find the meaning of the classification outcomes and to relate the results in the GSR signal response to a specific kind of stimuli. To solve this problem, an accurate feature selection and evaluation prior to classification is a necessary step to improve accuracy and reliability of emotion recognition systems. The aim of this study is to achieve a deeper knowledge on the characteristics of this promising signal and to select and evaluate which are the most significant features related to the GSR response, trying to minimise computational costs, by excluding redundant and irrelevant features. To this purpose, a wearable device, the Empatica E4 wristband, will be evaluated against a stationary prototype laboratory sensor, the Arduino UNO based GSR-Grove sensor, to also make a step toward the evaluation of wearable, unobtrusive devices, for real life applications.

This Thesis is structured as follows. In Chapter 2, a theoretical background about the GRS signal and some of the most used features are reported. Chapter 3 gives information about the two devices used for data collection. In Chapter 4, the experimental protocol used for

data acquisition, data processing and data analysis is reported. In particular, the study focused the attention on the use of different levels of physical exercise as stimuli. Both time domain and frequency domain features were evaluated. Experimental test results are presented in Chapter 5. Discussion and conclusion are reported in Chapter 6 and, finally, future developments are proposed in Chapter 7.

# Chapter 2

# State of the Art

## 2.1 Physiology of the skin and eccrine sweat glands

The skin is the largest organ of the human body and it is in contact with the external environment acting as a barrier. As it is part of the integumentary system, its main functions are protection and regulation of the body, in collaboration with all the other systems. Indeed, the skin is one important actor of the immune system because it gives the first life defence against infections and external agents. One of the main physiological mechanisms which are controlled by the skin is the thermoregulation: body temperature changes are possible thanks to sweat secretion, pilo-erection and peripheral circulation. In particular, our brain manages and regulates the heat loss by sending several nerve impulses to the skin in three different ways: skin hairs can trap more warmth if they are erected, and less if they are lying flat; glands under the skin secrete sweat onto the surface of the skin in order to increase heat loss by evaporation if the body needs to be cooled down; capillaries near the surface can open and close in order to dissipate or conserve heat respectively. Moreover, the skin is involved in perception as contains an extensive network of receptors for temperature, pressure, and pain to detect changes in the environment and relay based on the activity [9].

As shown in *Figure 2.1* the skin is composed by three main layers that are the epidermis, dermis and hypodermis. The epidermis is the outmost protective layer and it is composed of keratinized, stratified squamous epithelium not vascularized, with hardness and water-resistant properties. The dermis contains blood and lymph vessels, nerves, and other structures, such as hair follicles and sweat glands. The dermis is made by two layers of connective tissue that compose an interconnected mesh of elastin and collagenous fibres, produced by fibroblasts. It also acts as a cushion against stress and strain. The hypodermis consists of well-vascularized, loose, areolar connective tissue and adipose tissue which anchors to bone and muscles [10].

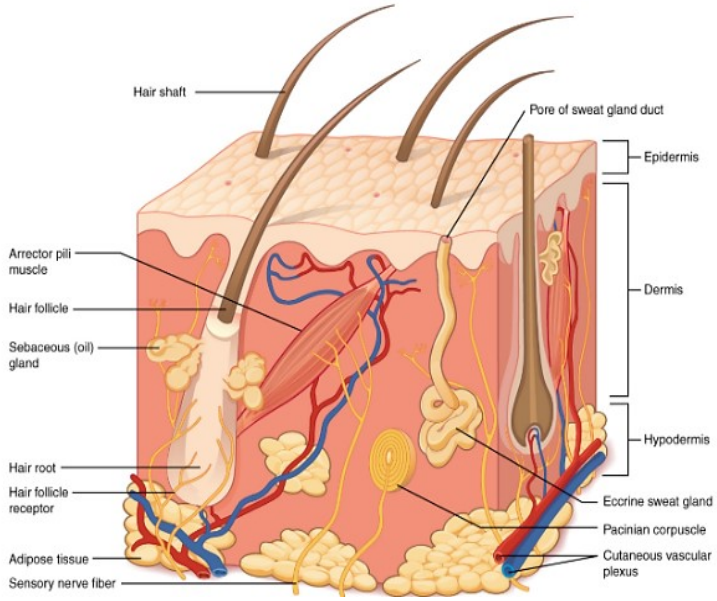


*Figure 2.1. Layers of the skin and eccrine sweat glands location.*

Among the 4 million sweat glands contained into the skin, almost 3 million ones are the so-called eccrine sweat glands, which are found in higher density on the soles of the feet, the forehead, the cheeks, the hand palms and the fingers. The fluid secreted by the secretory portion of eccrine glands is an ultra-filtrate one. Once the cells lining the duct portion reabsorb sodium from this liquid and conserves electrolytes it becomes hypotonic sweat. This change in the balance of positive and negative ions in the secreted fluid makes it possible for electrical current to flow more readily, resulting in measurable changes in skin conductance [9]. This change in skin conductance is generally termed as Galvanic Skin Response (GSR). Sweat secretion cannot be controlled consciously because it is driven by the Autonomic Nervous System (ANS). The ANS is subdivided into sympathetic and parasympathetic branches. The sympathetic nervous system represents a rapid response system for immediate motor action; therefore, it is also related to the "fight or flight" response. Increased sympathetic activity is associated with physical indicators of "autonomic arousal" such as increased heart rate, respiration rate, blood pressure, and sweating. The parasympathetic nervous system (PSNS) regulates processes associated with slow changes, the so-called "resting and digesting" or "feeding and breeding" response. The unconscious processes of sweat secretion reflect changes in arousal and therefore they are solely controlled by the SNS. Hypothalamic areas, especially the paraventricular and posterior nuclei but also many other subcortical and cortical regions are known to be

involved in the central control of sweat glands activity [11]. The thermoregulatory centre of the hypothalamus responds not only to changes in core body temperature, but also to hormones, endogenous pyrogens, physical activity, and emotions. Palm and soles sweating, in particular, seem to be linked with emotional sweating. The origin of emotional sweating could be explained from the ancestral need of humans of high gripping friction during hunting and fighting. As a result, palmar and plantar skin surfaces are more responsive to significant or emotional stimuli, as associated with the 'fight or flight' reflex [9]. The sympathetic fibres responsible for sweat glands stimulation are the sudomotor fibres, which descend via hypothalamic-reticular-spinal sympathetic pathways near other sympathetic efferences until ending at the preganglionic sudomotor neurons. Once the sweat has been discharged into the sweat ducts it passes through dermal and epidermal layers ending in a pore on the skin surface. Eccrine sweat glands cool down the body with the humidity deposition on top of the skin using sweat ducts. Nowadays the most accepted model of skin conductance change is the one proposed by Edelberg in 1972, for which the resistance of sweat ducts diminishes when the glands are stimulated through neurotransmitters and the pores are filled with sweat. When sweat fills the pores, the relatively resistant epidermal layer becomes more conductive. The higher the number of stimulated glands the higher the variation in skin conductance. More recently, in 1993, Edelberg proposed the "pore valve model", based on the hypothesis that intraductal hydraulic pressure could open pore ducts as valves and generate a sharp rising in the SCR. The hypothesis of this sweat accumulation in the pore valves could explain the rapid changes that occurs in the SCR [12]. Conduction time from central activation to the sweat glands of the fingertips has been estimated at 1.1 s to travel a mean distance of 1.1 m. Postganglionic sudomotor fibres are unmyelinated fibres with low conduction velocities between 0.5 and 2 m/s and each of these slow fibres innervates a skin area of about 1.28 $cm^2$. Vice versa each sweat gland is innervated by many different fibres. Microneurography studies have shown that sudomotor fibres fire in a burst fashion, with a mean duration of 638 ms per burst. Each burst corresponds to the temporal concurrence of multiple fibres firing together producing a single skin conductance response (SCR). The spike density in a single burst is reflected by the SCR amplitude recorded and is linearly related to the number of recruited glands and the frequency of action potentials. SCR amplitude is, therefore, an indicator of sympathetic activity [13].

## 2.2 GSR signal

GSR is also known as Skin Conductance (SC), Electrodermal Activity (EDA), Electrodermal Response (EDR), and Psychogalvanic Reflex (PGR). GRS signal can be decomposed into two main components, namely the tonic and phasic activity, associated with low and high frequencies respectively. Tonic activity is referred to as skin conductance level (SCL) and it corresponds to a slowly varying component which changes slightly in long periods from tens of seconds to minutes. These changes are related to the skin hydration level, which is under autonomic regulation, other environmental factors, stress levels of the subject and his physiology properties such as the thickness of the skin. This signal component is usually referred to as baseline, that differs across individuals. The phasic component instead shows fast variations occurring between one and five seconds after stimulus onset. This fast response is also called Skin Conductance Response (SCR) or orienting response (OR) and it is sensitive to emotional arousal evoked by a stimulus event, in that case, called event-related or specific SCR (ER-SCRs). If the phasic response happens spontaneously, because of internal or mental events, it is called non-specific SCR (NS-SCR) and it occurs at a rate of 1 to 3 per minute. An SCR appears as a superimposition of a small wave on the tonic component and shows a steep incline to the peak and a slow decline to the baseline. The succession of SCRs usually results in a superposition of subsequent SCRs, as one SCR arises on top of the declining trail of the preceding one [6][13].

There are wide individual differences in both tonic and phasic EDA related to demographic variables such as age, gender, and culture. For example, older adults are generally affected by lower tonic arousal levels and smaller phasic NS-SCR responses than young people. There is evidence that children less than 5 years of age exhibit smaller phasic changes than older children. The effects of age may be due to peripheral or central nervous system changes with age, or both. At the periphery, the number of active sweat glands is lower in older adults (mean age of 69.5 years) than in younger adults (mean age of 25.3 years), which may partially account for the lower tonic and phasic findings. Aging is also generally associated with a reduction of brain grey matter including important areas for electrodermal activity. Gender differences also have been noticed in tonic and phasic EDA trends, although the effects vary depending on the situation and the nature of the stimulus. In general, women show larger SCRs to unpleasant pictures than men as indicating that women respond with

greater defensive activation than men to affective pictorial stimuli, although exceptions have also been found. Anyway, whether gender differences in EDA reactivity are due to sociocultural or biological differences, or both, is yet to be determined. In contrast to unpleasant stimuli, men and women respond similarly to pleasant pictures except for erotic stimuli, where men show significantly larger SCRs than women. Ethnic differences have also been observed in EDA. For example, early research found lower SCL in African American children (mean age 7 years) and adults (mean age 22.9 years) than in age-matched Caucasian American children and adults. The fact that there was no ethnic difference in other measures (EEG, heart rate, skin temperature, blood pressure, frequency of NS-SCRs) led the researchers to suggest that the basal EDA difference was due to peripheral effects such as the thickness of the epidermal layers or the number of active sweat glands. A subsequent research has replicated the finding of lower SCLs among African Americans and generally, but not always, confirmed a lower density of active sweat glands. Certain external environmental variables such as temperature and humidity have been investigated as sources of variance in EDA. All in all, although palmar eccrine sweat glands are not as sensitive to temperature as those found in other body sites, they are still influenced by temperature. Correlation with the change in relative humidity is still controversial [14].

## 2.3 GSR device

The main components of a GSR device are usually three: two electrodes attached to the skin to apply constant voltage/current and to measure skin conductance/resistance, the amplifier for signal conditioning and the Analog to Digital Converter (ADC) to allow the signal recording and storage into binary data. Real-time visualization of signal recording is then possible on the screen of a computer or smartphone app. In the case of wireless devices, a Bluetooth connection can allow for data streaming visualization and uploading more comfortably and easily.

### 2.3.1 GSR Sensors

GSR sensors are usually electrodes of Ag/AgCl with a measurement site of about 1 $cm^2$. The sensing site can be embedded in adhesive patches, Velcro straps, or finger clips to be easily positioned in the desired skin site and connected utilizing a press button connector to the cables of the electrodes. In case of disposable adhesive gel electrodes, the main disadvantage is that they are single usage and they require gel, but they have the advantage to give a better signal quality than dry Velcro straps and finger clips, and they can be applied in many different sites, not only on fingertips. Another option is the use of electrodes embedded on elastic straps that can be placed around the wrist, the arm or the fingers, depending on the size. Finally, there are electrodes embedded in rigid wristbands, smartwatches or rings that allow for wireless measurements and can be used in a large variety of daily activities [15].

The highest sweat gland density is found in the palms of the hands, fingers, foot soles and toes. Indeed, these represent the most common sensor placement sites and are chosen relative to the application and tasks that the subject should perform. The wrist is also chosen for its high versatility to be used in wearable devices.

## 2.4 Data acquisition

Different methods of EDA recording have been developed and tested over time and have been applied in many studies, but nowadays two different methods of measuring EDA exist. The exosomatic method, applying direct current (DC) or alternating current (AC) using electrodes, and the endosomatic method performed without applying external current. In the exosomatic method, one electrode is placed on the active site and a reference electrode at a relatively inactive site. The measured potential is similar, but it has a more complex response than endosomatic methods. In DC measures, when tension is maintained constant, the current flow follows the Ohm's law I=V/R and it is proportional to 1/R, where R is the resistance of the skin. The reciprocal of the resistance is also named conductance and it is measured in Siemens (S) where 1 S equals 1/Ohm. To measure the current, a small resistor is placed in series with the skin and the voltage drop across this series resistor is monitored. Applying Ohm's law for a second time, since the value of the resistor is known, the voltage

drop is proportional to the current and consequently, it is proportional to the conductance. This way, it is possible to measure the skin conductance by applying a constant voltage. The same procedure can be obtained by applying a constant current to the skin, to measure the skin resistance but making sure that the applied current is low enough to ensure the safety of sweat glands. In AC measures, a more complex comprehension of mathematics is required, but in general, it is possible to obtain measures of the skin impedance (SZ) if a constant current is applied, or skin admittance (SY) in the case of constant voltage. This is possible because the skin membranes behave like capacitive elements capable to store energy. SZ is measured in Ohm while SY in Siemens. As the skin resistance is in the order of MOhm, the conductance is usually expressed in μS [14].

The choice of the sampling frequency is up to the user, but in general, relatively low sampling frequencies are enough for GSR only recording applications, which don't need to record other slowly varying signals such as acceleration or heart rate. In general, frequencies lower than 10 Hz are suggested [7]. Higher frequencies could allow having minor discontinuities in GSR range changes, but they do not have any effect on GSR data which has a much lower frequency range of interest.

### 2.4.1 Noise and artefacts

GSR recording is affected from different sources of noise and artefacts that, ifnot removed before signal analysis, can be subjected to misinterpretation and considered as true Skin Conductance Response (SCR). In case of AC recording, the powerline noise could add an artefact that is easily removable with low-pass filtering, being the typical EDA frequency range much lower than the AC frequency input (i.e. typically 50 or 60 Hz). SCL baseline signal could present shifts in the skin conductance caused by changes in sensor positioning due to motion. This is crucial when data are collected from wearable devices because motion artefacts can affect the signal. In the same way, changes in the amount of contact surface of the sensor with the skin can occur during motion and produce jump discontinuities in the skin conductance. Excessive pressure of the electrode or adjustment of the device is also reflected in the recording. Muscular activity in non-recording locations, is another important source of noise. Physiological signal changes such as respiration, temperature and heart rate variations also modify the signal. For example, talking during the recording can add slow variations to the signal that are not to be taken as GSR components [14].

### 2.4.2 Respondent instructions

The best way to limit the presence of artefacts is to perform a correct sensor placement and give some instructions to the subjects. Sensors should stay firmly connected to the skin throughout the experiment, always in the same skin location for all subjects. To improve sensor stability in subjects with oily skin, cleaning with an alcohol solution is recommended. Additionally, subjects should be informed to avoid deep breaths, limb movements and talking. Before starting the recording, they should find a natural comfortable position [7].

## 2.5 Data analysis

The data analysis is intended to evaluate the specific SCRs characteristics that are different for everyone. Each subject has a different baseline due to different physiological characteristics and to the environmental conditions at which the recording is performed. This baseline should be collected to have the possibility to separate it from the real skin conductance response to a stimulus. Individual SCRs, interpreted as a direct measure of arousal, can be characterized by the following four parameters [7] [16]:

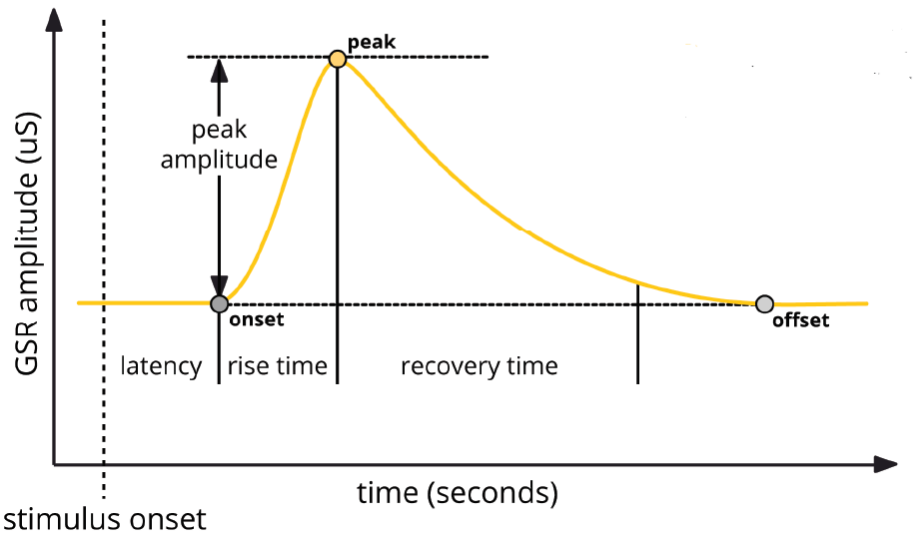


*Figure 2.2. SCR parameters.*

1. Latency: the time between the stimulus and the onset of the phasic burst. The signal deflections from the baseline are attributed to the stimulus only if they fall in a predefined response window that is typically 1–3 s or 1–5 s. The onset is set to a point to which a minimum amplitude criterion from 0.01 to 0.05 μS is often applied. Changes that occur before the latency are considered NS-SCRs.

2. Peak amplitude: the difference between the SCR peak and the amplitude onsets. The minimum is usually set at 0.05 μS.

3. Rise time: the time between the onset and the peak of the SCR.

4. Recovery time: the time from the peak to reach a complete recovery.

While the onset of an SCR can be quite steep, the recovery is typically flatter, resulting in longer recovery times.

### 2.5.1 Signal processing

The raw GSR data is usually sampled at a higher sampling frequency than required and can be down-sampled without losing important information. Frequencies below 10 Hz are enough to capture all the information contained in the GSR signal, which is confined in the frequency band [0-0.5] Hz [17]. Filtering procedures are used in order to separate and extract the phasic component from the tonic component, since the phasic component is related to slightly higher frequencies with respect to the tonic one and is usually analysed to measure the SCR. Filtering the signal is not the only way to extract the SCRs, since also Linear Interpolation, Curve Fitting, through-to-peak methods or signal decomposition approaches such as Continuous Decomposition Analysis and Discrete Decomposition Analysis can be used [1][11]. To quantify SCR signals, then, the SCR parameters are used to implement automatic detection algorithms capable to extract peak amplitudes and to count the number of GSR peaks. Peak amplitude and number of peaks are two of the more used metrics for the quantification of emotional response, but algorithms to extract these features are computationally demanding and does not give any information on the kind of stimuli related to the response. Nowadays, a high number of new features are being tested to quantify the SCR signal but also to try to relate the response to different kind of stimuli. Positive results in this approach could allow the use of GSR signal for the implementation of emotion

recognition systems. An overview of the GSR features mainly investigated is reported in the next paragraph.

### 2.5.2 Features selection

Recent research has investigated the predictive power of diverse types of GSR features. Most frequently used features in the time domain are statistical descriptive features such as signal mean value, standard deviation, kurtosis, skewness, and variance [8][18]. Other metrics that were frequently encountered in the literature were related to morphological alterations in the signal such as for the area under the curve. Further features extracted involve the computation of the first derivative of the signal, mean of the first derivatives and the mean of the negative first derivatives are two of the most proposed [19]. Few researches have focused on frequency domain features, but since the transient characteristics of the GSR signal affect principally the time domain, computing features on the Fast Fourier Transformed signal is considered a promising approach. Statistical aspects such as signal magnitude area, range, kurtosis, skewness, mean value, energy and entropy have been proposed [8]. All these metrics have been selected in the literature to be used as input for emotion recognition classification algorithms.

# Chapter 3

# Materials

The devices used in the study are the Arduino UNO based Grove-GSR Sensor and the wireless Empatica E4 wristband.

## 3.1. Arduino UNO based Grove-GSR Sensor

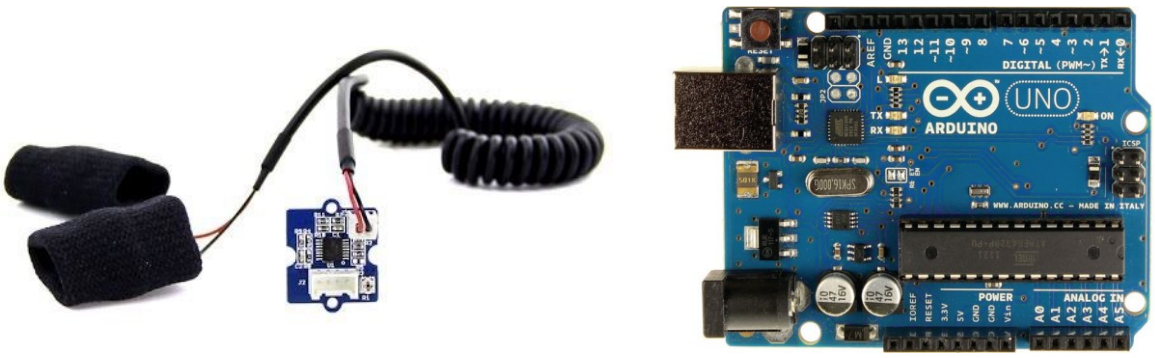


*Figure 3.1. GSR-Grove Sensor (left) and Arduino Uno board (right).*

The GSR-Grove Sensor v1.2, shown in *Figure 3.1*, is designed to record skin resistance, by wearing two elastic bands, equipped with two embedded electrodes, on the fingers. Sensor specifications are reported in *Table 3.1*.

*Table 3.1*. GSR-Grove sensor specifications.

| **Parameter** | **Value/Range** |
|---|---|
| Operating voltage | 3.3V/5V |
| Sensitivity | Adjustable via a potentiometer |
| Input Signal | Resistance, NOT Conductivity |
| Output Signal | Voltage, analog reading |
| Finger contact material | Nickel |

A Groove cable is used to connect the GSR sensor to the Arduino UNO board. There are four coloured wires: pin 1 is yellow and corresponds to the first analog input, pin 2 is white and corresponds to the second analog input (not used), pin 3 is red and corresponds to the power for Grove Module (VCC 5V/3.3V) and pin 4 is black and corresponds to Ground (GND). To set up the sensor, the pin 1 is connected to the analog input A0 of the Arduino UNO board, pin 3 is connected to the 5 V voltage supply and pin 4 to the 0 V ground. The Arduino UNO board is connected to the PC via USB for data transfer, and programmed with the following code:

```
const int GSR=A0;
int sensorValue=0;
int gsr_average=0;

void setup(){
  Serial.begin(9600);
}

void loop(){
  long sum=0;
  for(int i=0;i<20;i++)
      {
      sensorValue=analogRead(GSR);
      sum += sensorValue;
      delay(5);
      }
   gsr_average = sum/20;
   Serial.println(gsr_average);
}
```

The code presented above, initializes the integer variables, sets the velocity of data transfer at 9600 bit per second (bps) and measures the value of the pin A0. Moreover, to remove the glitch, the code computes the mean signal level every 20 measurements, delaying 5 milliseconds one from the other, and prints the obtained data on the serial port with a sampling rate of 10 Hz. In order to obtain the maximum possible excursion for the input signal measured, the calibration steps provided the GSR Pocket Guide delivered by iMotions [7] were followed. Therefore, the onboard potentiometer of the Grove module is adjusted using a screwdriver, until the serial output of Arduino displays the half of the maximum value generated by the Analog to Digital Converter (ADC), corresponding to 512. According

to the sensor datasheet, to convert the values output by the ADC into Human Resistance (HR) values, the following formula has to be applied:

HR = ((1024 + 2 * Serial Port Reading) * 10000) / (512-Serial Port Reading) [Ω]

where Serial Port Reading is the ADC value shown in the Serial Port (between 0 and 1023).

## 3.2 Empatica E4 Wristband

*Figure 3.2. Empatica E4 Wristband.*

The E4 wristband by Empatica, shown in *Figure 3.2*, is a medical-grade wearable device that allows real-time unobtrusive acquisition of physiological data. The E4 is equipped with four different sensors for the recording of biometric parameters:

- a Photopletismographic (PPG) sensor that measures Blood Volume Pulse (BVP) and from which the Heart Rate Variability (HRV) is derived,
- a three-axis accelerometer that captures activity based on motion,
- an EDA sensor which measures changes in the electrical properties of the skin,
- an infrared thermopile that records peripheral skin temperature.

The wristband is provided with an internal real-time clock that is necessary for data synchronization and a single button that is used to power on and off the device, to reset and,

if used during the recording session enables to tag an event. Once the registration is launched, the E4 performs an initial automatic calibration phase for sensors calibration that lasts 10 to 15 seconds. An internal memory allows the recording mode of up to 60 hours of measurements, that can be transferred to the PC via USB, using the application called *E4 manager*. Data can also be acquired in streaming mode via Bluetooth using the mobile app, named *E4 realtime*. After each recording session, data are automatically uploaded to the cloud platform called *E4 connect*, where it is possible to visualise and download raw data related to the users in CSV format. Downloaded data are compressed in a ZIP directory containing the following files: ACC.csv file contains three-axis accelerometer sensor data sampled at 32 Hz in the range [-2g, 2g], BVP.csv file contains PPG sensor data sampled at 64 Hz, EDA.csv file contains data from the electrodermal activity sensor in μS and sampled at 4 Hz, IBI.csv file contains Inter Beat Intervals obtained from the processing of the BVP signal with an algorithm that already removes incorrect peaks due to noise in the BVP signal, TEMP.csv file contains temperature sensor data expressed in degrees on the Celsius (°C) scale and sampled at 4 Hz, HR.csv file contains the average heart rate values, derived directly from the BVP with 1 Hz sampling rate, and info.txt file contains the descriptions of the files [20]. Technical specifications are reported in *Table 3.2.*

*Table 3.2*. Empatica E4 wristband specifications.

| **Parameter** | **Range/Value** |
|---|---|
| Form Factor | Case: 44x40x16 mm<br>Wrist: 110 - 190 mm<br>Weight: 25 g |
| Battery | Streaming mode: 24+ h<br>Recording mode: 32+ h<br>Charging time: < 2 h |
| Data Transfer | Bluetooth Low Energy Smart®<br>USB 2.0 |
| Flash Memory | Up to 60h of data storage |
| Splash Resistant Materials | Band: polyurethane<br>Case: polycarbonate and glass fiber<br>Lenses: polycarbonate and silicon |

# Chapter 4

# Methods

## 4.1 Data acquisition

EDA measurement data were acquired from four healthy subjects (2 males and 2 females) aged between twenty and sixty years. For each individual, three different recording sessions (at rest, after mild exercise and after intense exercise) were acquired in three different moments of the day (morning, afternoon and evening) for a total of nine sessions per subject. This was done in order to have different repetitions of the same type of physical activity, so that the recording did not depend on the time of day it was acquired. Depending on the activity to perform, the acquisition time was different. Sessions at rest lasted 15 minutes, while the subject was lying on a bed. Then, subjects were asked to perform almost 5 minutes of mild exercise consisting of walking and climbing stairs. As soon as the exercise was over, the subjects were asked to lie down on a bed to acquire a 10-minute recording. The same was done to acquire 10-minute recordings after almost 5 minutes of intense exercise that consisted in running stairs or performing repetitions of a fatiguing free body exercise. Exercises were chosen basing on the guidelines provided by the Mayo Clinic website [21]. Subjects' details are reported in *Table 4.1*

*Table 4.1. Subjects' details.*

| | **Age** | **Male(M) / Female (F)** | **Left (L) / Right (R) handed** |
|---|---|---|---|
| Subject 1 | 25 | F | R |
| Subject 2 | 30 | M | R |
| Subject 3 | 59 | F | R |
| Subject 4 | 20 | M | R |

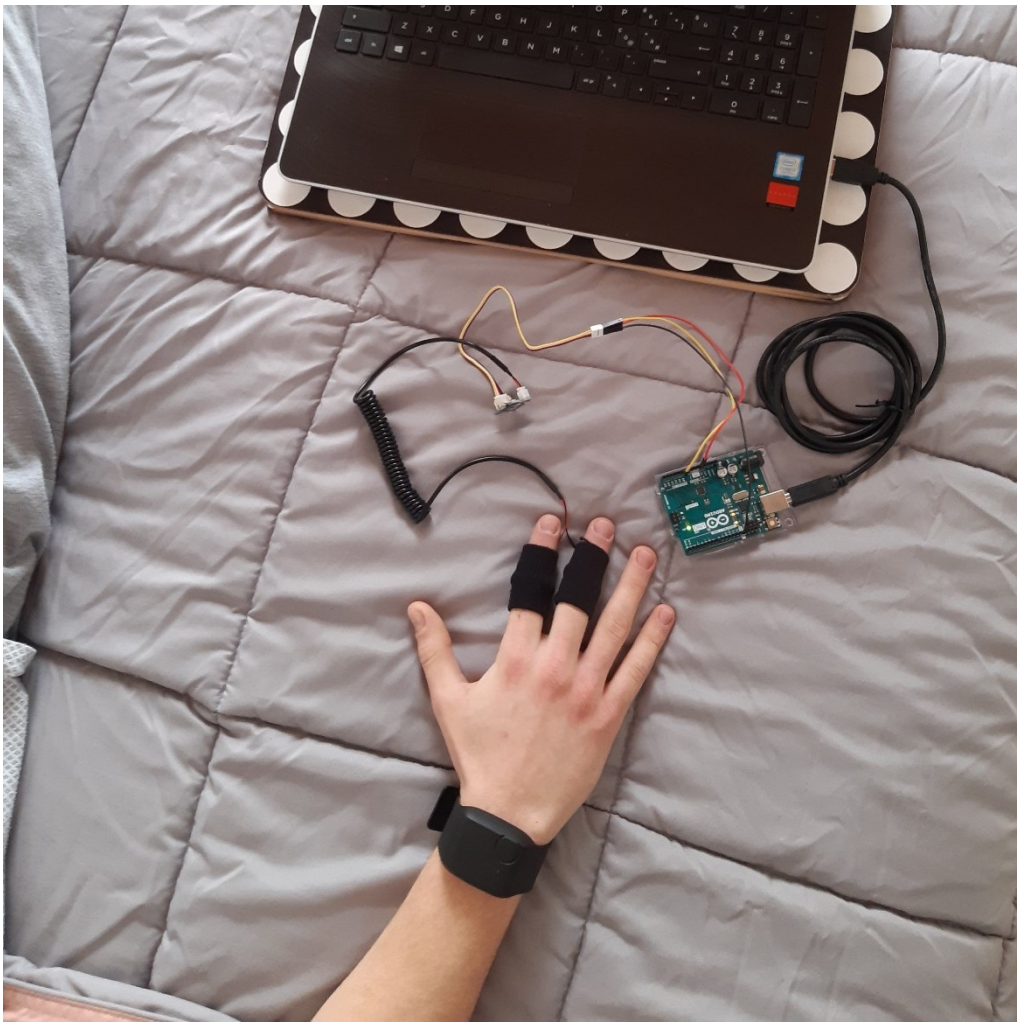

*Figure 4.1. Sensors positions setup.*

EDA signals were recorded both with the Grove-GRS Sensor connected to the Arduino UNO board and with the Empatica E4 wristband, simultaneously. The positioning of the sensors, shown in *Figure 4.1* took place at the end of the various physical exercises and no exercises were performed wearing the sensors. This was done in order to avoid wetting the electrodes with an excessive amount of sweat. The E4 sensor was placed at the participant dominant wrist, that for all of them was the right wrist, since there is evidence from the literature that GRS data acquired from the dominant limbs usually give higher amplitudes. The Grove-GSR elastic bands were positioned on the middle phalanxes of both the index and middle finger of the dominant hand, enabling the appropriate contact of the electrodes with the fingertips. In fact, to guarantee accurate measurements, the sensors were regulated and positioned in such a way to be well attached to the skin throughout the experiment. Data were acquired in a quiet room without the presence of visual or auditory stimuli. To minimize the artefacts and deterioration of data quality, the subjects were instructed to try not to talk

and breathe normally because excessive inhalation and exhalation could affect the GSR, with drifts in the signal. Other instructions regarded the limited movements of body, especially where sensors were attached. To facilitate the fulfilment of these indications, subjects were provided with a bed to lie on, in a natural position, and were asked if they were feeling comfortable. Before starting the recordings, it was ensured that all the Grove-GSR Sensor and Arduino configuration cables were correctly connected and that the wireless E4 wristband was charged and within the Bluetooth reception range of the mobile phone, without obstructions in between. GSR measurement data from Grove-GSR sensor were collected by using the *CoolTerm* Serial Port Terminal Software and saved in .TXT files. Before collecting data, the structure of these files was defined by uploading a code into Arduino IDE platform. In particular, the format was structured in two columns, the first containing timestamps in the format HH:MM:SS:sss with millisecond resolution, and the second one containing ADC signal values to be converted into human resistance values (Ohm). E4 recordings were acquired in streaming mode using the *E4 realtime* app and then downloading the CSV files from the *E4 connect* online platform. For a possible future use of the dataset in subsequent studies, the subjects were asked to fill a questionnaire, based on the Self-Assessment Manikin (SMA) scale [22], which is used in many studies of EDA signal to get feedback from the subjects about their feelings during the recording session. The subject had to indicate for each recording session the level of valence and of arousal that mostly resembled his emotional status during the recording. The SAM scale is reported in *Figure 4.2.*

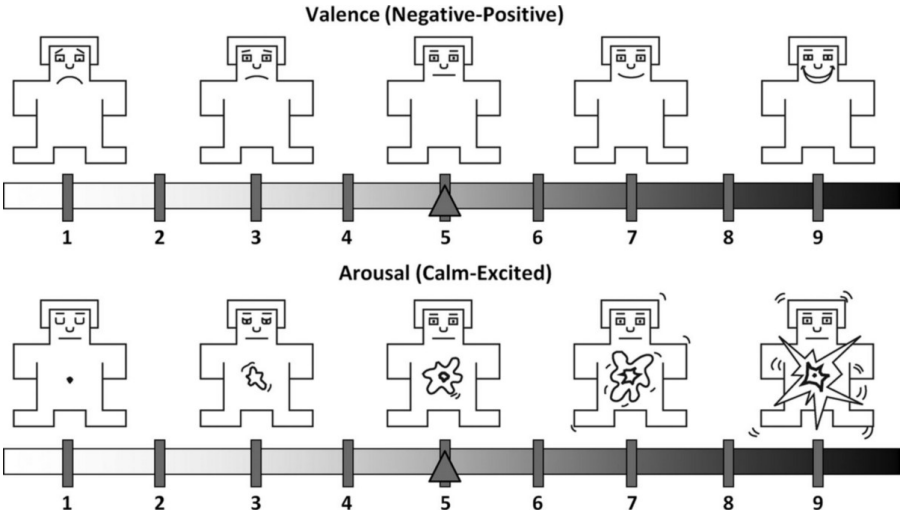


*Figure 4.2. SAM scale.*

Valence accounts for the positivity/negativity of the emotion, while arousal for the level of excitement. High valence and arousal values correspond to positive emotions such as happiness and joy, high valence and low arousal values are related to a relaxed and calm emotional status, low valence and high arousal are perceived in case of negative emotions such as anger, fear and stress and, finally, low valence and low arousal values includes negative emotions such as sadness and depression.

## 4.2 Data processing

Once data acquisition was concluded, data were imported in MATLAB to be processed and analysed. As a first step the samples corresponding to the first 30 seconds and last 30 seconds were removed from the recordings with a subtraction algorithm, in order to reduce errors due to initial and final transient events in the signal, such as electrode skin coupling and sensor calibration or expectance induced responses. After that, to make the simultaneously recorded tracks comparable, raw data acquired with the Grove-GSR sensor were pre-processed. In particular, the formula of the HR provided from the sensor datasheet was applied to obtain skin resistance values in Ohm. Then, since Empatica E4 measures data in micro Siemens (μS), a conversion from Ohm to μS was applied to the Grove-GSR data to obtain Skin Conductance (SC) values. Since the conductance is the reciprocal of resistance, the applied formula was as follows:

Skin Conductance [μS] = 10^6*(1/Skin Resistance [Ohm]).

Similarly, the sampling frequency of the Grove-GSR sensor was modified. Specifically, to obtain the same sampling frequency for both the recordings, the Grove-GSR measurements were down-sampled from 10 Hz to the same sampling frequency of Empatica E4 (i.e. 4 Hz). The MATLAB function *resample* was used to downsample the input sequence at 2/5 times the original sample rate of 10 Hz. This function applies an antialiasing FIR low-pass filter to the input sequence and compensates for the delay introduced by the filter.

### 4.2.1 Signal decomposition

In order to separate the tonic and phasic components, a basic median filter was designed. The following piece of code was used:

```
for i = 17 : length(signal)-16
        tonic_sample(i) = median(signal(i-16 : i+16));
        phasic_sample(i) = signal(i)- tonic_sample(i);
end

    tonic_signal = tonic_sample(17 : end) ;
    phasic_signal = phasic_sample(17 : end) ;
```

Index *i* was used to go through the data sample by sample. For each sample the median was computed in a +4/-4 seconds time interval. By considering the sampling frequency at 4Hz, 4 s correspond to a window centred in *i*, including 16 samples before and 16 samples after the current $i^{th}$ sample. The so computed median value replaced the central value in the new generated vector *tonic_sample*, which represents the tonic component of the signal. Then, this component was subtracted from the initial signal to extract the phasic component, generating the vector *phasic_sample*. Out of the *for* cycle, the first 17 samples of each obtained component were cut because all equal to zero. An example is reported in the *Figure 4.3*.

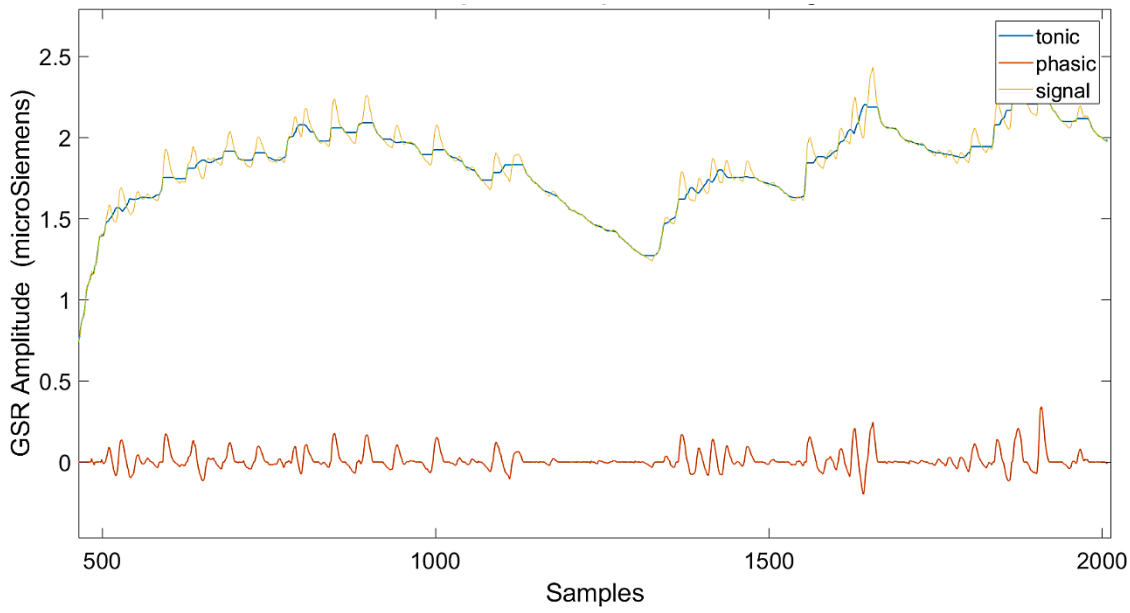


*Figure 4.3. Example of a signal (yellow) with phasic (red) and tonic (blue) components extracted applying a basic median filter in the time domain.*

### 4.2.2 Frequency analysis

For frequency analysis, the Fast Fourier Transform (FFT) magnitude of both phasic and tonic components was computed for Grove-GSR and Empatica E4 measurement data, using the MATLAB *fft* function. An example of FFT magnitude of tonic and phasic components related to E4 and Grove-GSR sensors is reported in *Figure 4.4*.

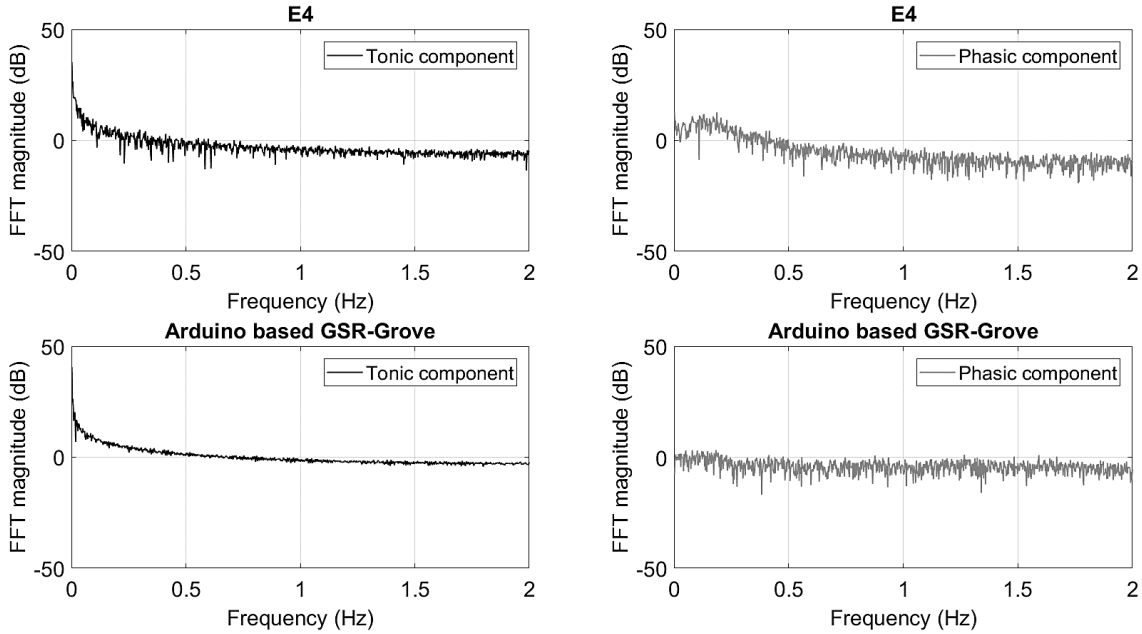


*Figure 4.4. Example of FFT magnitude of tonic (black) and phasic (grey) components related to the E4 (upper panels) and GSR-Grove (lower panels) sensors in frequency domain.*

### 4.2.3 Features extraction

The choice of the features that were extracted from the recorded data was made based on the features that appeared more frequently in the literature, as confirmed in a review article about EDA features selection and extraction [8]. It was decided to compute metrics both in time and in frequency domain. Within the time domain, the features selected were:

- Mean value: also called the mathematical expectation or average, is the central value of a discrete set of numbers, computed as the sum of total samples $x_i$ divided by the signal length (number of samples $n$).

$$\overline{x} = \frac{1}{n}(\sum_{i=1}^{n} x_i)$$

- Area Under the Curve (AUC): obtained computing the approximate integral of the signal using the trapezoidal method, which performs numerical integration. This approach approximates the integration over an interval by breaking the area down into trapezoids with more easily computable areas.

$$\int_a^b f(x)dx \approx \frac{b-a}{2N}\sum(f(x_n)+f(x_{n+1}))$$

where $\frac{b-a}{2N}$ is the spacing between two points.

- Variance: computed as the normalized sum of the square difference between each sample and the mean value.

$$V = \frac{1}{N-1}\sum_{i=1}^{N}|x_i-\mu|^2$$

where $\mu$ is the mean of the signal.

- Standard Deviation (STD): measure of the dispersion or variation from the mean of the signal obtained with the square root of the variance.

$$\sqrt{V}$$

- Kurtosis: Measure of the distribution shape around a normal distribution

$$k = \frac{E(x-\mu)^4}{\sigma^4}$$

where $\mu$ and $\sigma$ are the mean and the standard deviation of the signal respectively, and E represents the expected value.

- Skewness: it measures the asymmetry of the data distribution around the mean value. If skewness is negative, the data spreads out more to the left side of the distribution graph (values lower than the mean). If skewness is positive, the data spreads out more to the right side (values higher than mean).

$$s = \frac{E(x-\mu)^3}{\sigma^3}$$

where $\mu$ and $\sigma$ are the mean and the standard deviation of the signal respectively, and E represents the expected value.

- Mean Derivative: is the mean of the first order derivative of the signal.

$$\overline{d} = \frac{1}{n}(\sum_{i=1}^{n} \frac{\Delta x_i}{\Delta t_i})$$

where $n$ is the number of samples, $x$ is the signal, $t$ the signal sampling time and $\frac{\Delta x_i}{\Delta t_i}$ are computed with the MATLAB function *diff*.

- Negative Mean Derivative: is the mean of the first order derivatives of the signal with negative values, computed considering only negative derivatives.

The frequency-domain features were extracted from the FFT signal magnitude. Similarly to the procedure followed in time domain, the features computed in frequency domain were:

- Mean value
- Signal Magnitude Area (SMA): computed with the same function used for the AUC in time domain.
- Range: computed as the difference between the maximum and minimum values among all the samples of the signal.
- Standard Deviation (STD)
- Kurtosis
- Skewness
- Energy: also called total power energy is defined as the area under the squared magnitude of the considered signal and is computed with the sum of each squared FFT coefficient.

$$s = \sum_{i=1}^{n} FFT_i * FFT_i^*$$

where $FFT$ is computed with the *fft* MATLAB function and $FFT_i^*$ is the complex conjugate of $FFT_i$.

- Entropy: is a statistical measure of randomness that is computed as the negative of the sum of the probability multiplied by its logarithm, where the probability is given by the power energy of each coefficient divided by the total power energy.

$$H = \sum_{i=1}^{n} p \log(p)$$

where p is derived from the energy and is equal to $p = \frac{s}{\sum_{i=1}^{n} s}$.

Features were extracted using a MATLAB code. Both time domain and frequency domain features were computed for each one of the two GSR components, tonic and phasic, and separately for the data relative to the different sensors.

### 4.3.4 Data reduction

In order to manage the big amount of data collected for the experiment and to reduce its complexity, a data reduction protocol was designed and implemented on the entire dataset. This was necessary to have a better overlook on the results and to make interpretations easier. The protocol was executed separately for the data collected with the two different sensors and for the features computed on the tonic component of the signal and for those computed on the phasic one. The first step consisted in the averaging of the computed feature values related to the same subject and to the same physical activity. This way, the feature values obtained from Morning, Afternoon and Evening sessions were reduced to a single average value. This was done for all the features. The second step was the normalization of data related to the same feature across all the subjects. The maximum value that a certain feature reached was used to normalise the entire set of data related to that feature, to get values included in the range [-1, 1]. Then, the last step consisted in the evaluation of the discrepancy among the same feature computed for the two different GSR components. This was done computing a *delta* between the value of the feature obtained for the tonic and for the phasic component. This *delta* was computed as follows:

$\Delta_{\text{Feature}} = \text{Feature}_{\text{tonic}} - \text{Feature}_{\text{phasic}}$

where $\Delta_{\text{Feature}}$ is the difference between the normalised values of the feature, and $\text{Feature}_{\text{tonic}}$ and $\text{Feature}_{\text{phasic}}$ are the normalised values of the feature computed on the tonic and on

the phasic component respectively. The obtained delta values were compared to a threshold in order to consider significant only those variations that were higher than the 50%, hence, where $\Delta_{Feature}$ absolute value was higher than 0,5. Features for which the $\Delta$ overcame that threshold were considered significant, concerning the subject and physical activity they were related to. These results were summarised filling a table for each feature. An example is reported in *Table 4.2.*

*Table 4.2.* $\Delta_{50\%}$ *for the mean value.*

| Subject/Activity | Rest | Medium | High |
|---|---|---|---|
| Subject 1 | / | / | E |
| Subject 2 | A | A | A/E |
| Subject 3 | / | A | / |
| Subject 4 | / | A | A |

In each table an "A" was reported if the significant variation was observed in the feature computed for the Arduino UNO based GSR-Grove sensor, an "E" in the case the variation of at least 50% was observed in the E4 sensor, and "A/E" if was observed in both the sensors. . In tables' rows the subjects were reported, and the level of physical activity in the columns, to make, at the same time, comparisons on different aspects.

# Chapter 5

# Experimental Test Results

This chapter presents a description of the experimental tests with the relative results. The GSR measurement data of the 4 subjects involved in the experiments have been acquired and processed following, respectively, the procedure and the algorithms described in Chapter 4. In *Table 5.1* all the characteristics of the recording sessions acquired for each subject are listed. From the Table it is also possible to evidence that the dataset is composed by 3 sessions (i.e. Morning, Afternoon and Evening) for each exercise intensity (i.e. rest, medium and high), so as to have 9 registrations per subject. Since each session was recorded simultaneously with two sensors, the Arduino UNO based GSR-Grove sensor and the E4 wristband, a total of 72 registrations were saved.

*Table 5.1. Dataset characteristics.*

| **Subject** | **Exercise intensity** | **Duration (minutes)** | **Sessions: Morning (M), Afternoon (A), Evening (E)** | **Sensor** |
|---|---|---|---|---|
| Subject 1 | Rest | 15 | M, A, E | GSR-Grove, E4 |
| | Medium | 10 | M, A, E | GSR-Grove, E4 |
| | High | 10 | M, A, E | GSR-Grove, E4 |
| Subject 2 | Rest | 15 | M, A, E | GSR-Grove, E4 |
| | Medium | 10 | M, A, E | GSR-Grove, E4 |
| | High | 10 | M, A, E | GSR-Grove, E4 |
| Subject 3 | Rest | 15 | M, A, E | GSR-Grove, E4 |
| | Medium | 10 | M, A, E | GSR-Grove, E4 |
| | High | 10 | M, A, E | GSR-Grove, E4 |
| Subject 4 | Rest | 15 | M, A, E | GSR-Grove, E4 |
| | Medium | 10 | M, A, E | GSR-Grove, E4 |
| | High | 10 | M, A, E | GSR-Grove, E4 |

An initial comparison among the GSR raw data can be done by visual inspection. The MATLAB plots of the signals of all the subjects, and related to the three exercise intensities, are shown in *Figures 5.1-5.4*. Arduino UNO based GSR-Grove signals are shown after downsampling to 4 Hz in order to be comparable with E4 signals. Moreover, to facilitate the comparison and to be more consistent in the computation of the features, all the signals have been cut to the same length, corresponding to 8,5 minutes.

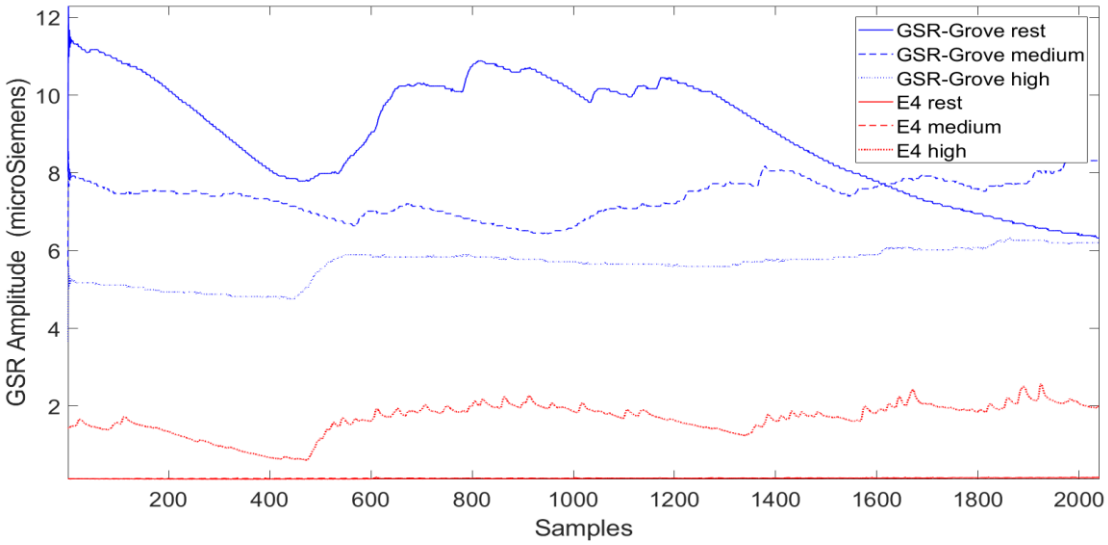


*Figure 5.1. Example of signals relative to Subject 1.*

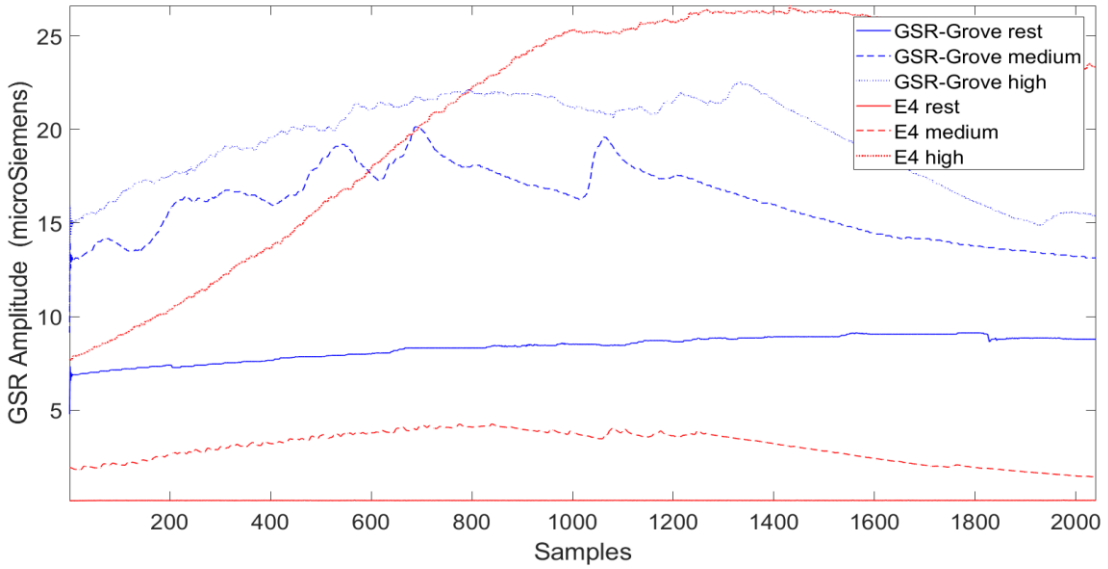


*Figure 5.2. Example of signals relative to Subject relative to Subject 2.*

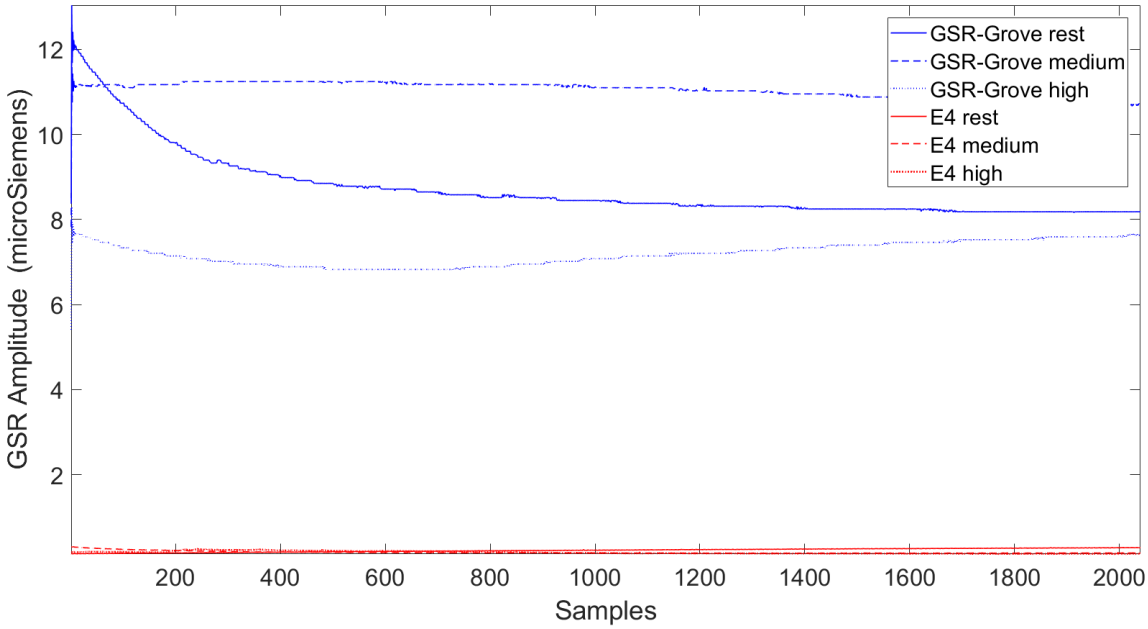


*Figure 5.3. Example of signals relative to Subject 3.*

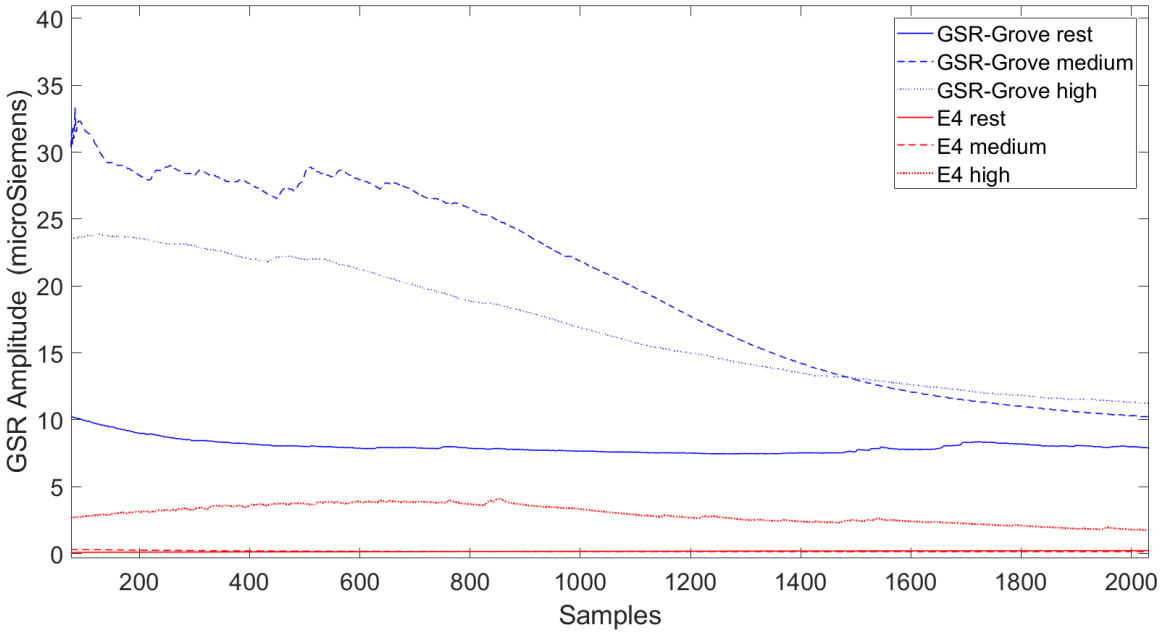


*Figure 5.4. Example of signals relative to Subject 4.*

In *Figures 5.5-5.12* Arduino UNO based GSR-Grove signals and E4 signals have been separated in two graphs, since the two sensors have different ranges and a single graph does not allow to have a good visual inspection.

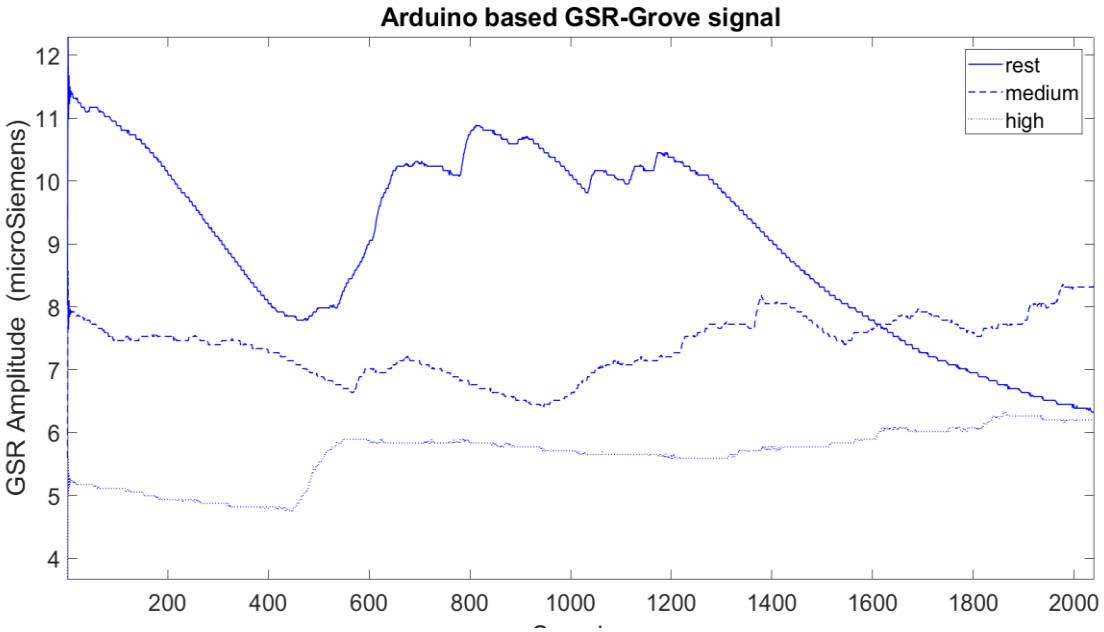


*Figure 5.5. Example of Arduino UNO based GSR-Grove signals relative to Subject 1.*

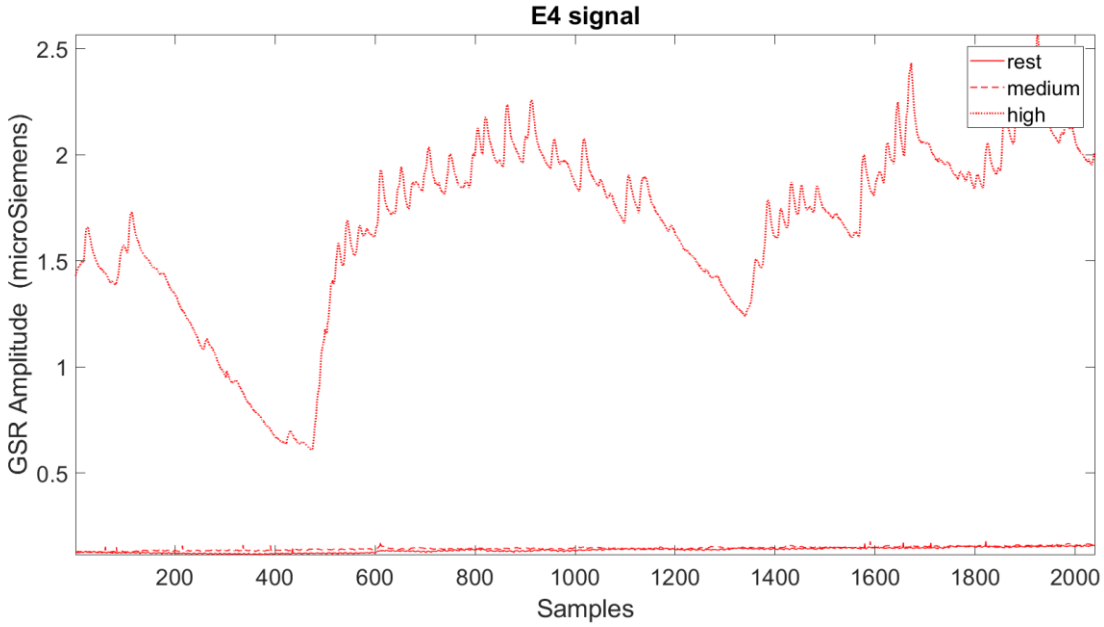


*Figure 5.6. Example of E4 signals relative to Subject 1.*

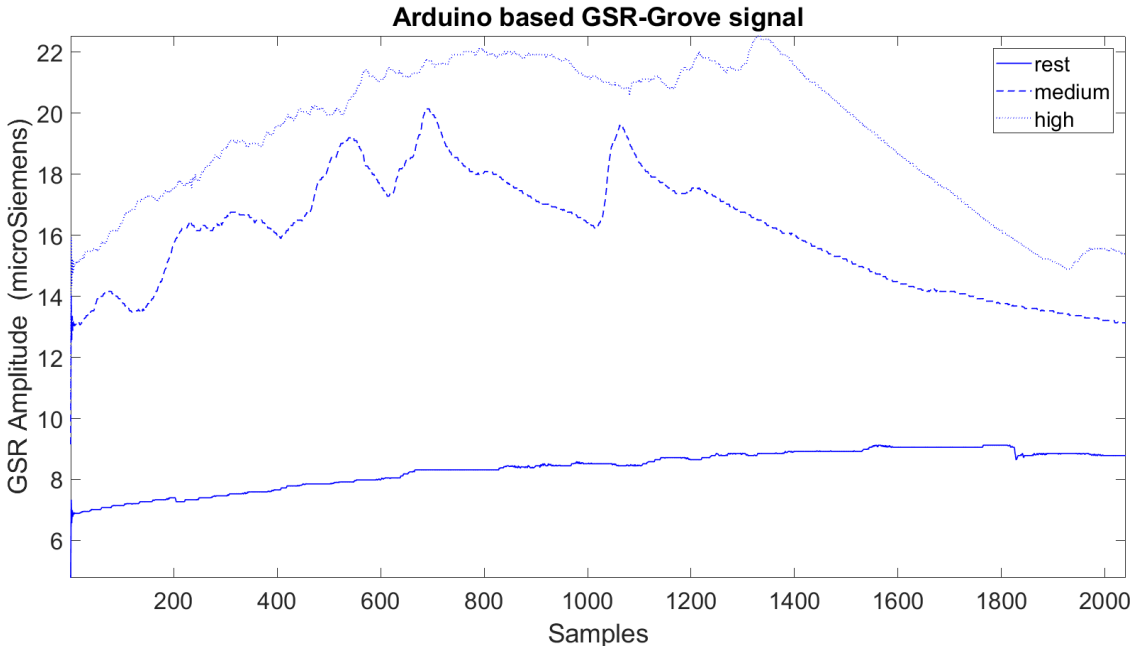


*Figure 5.7. Example of Arduino UNO based GSR-Grove signals relative to Subject 2.*

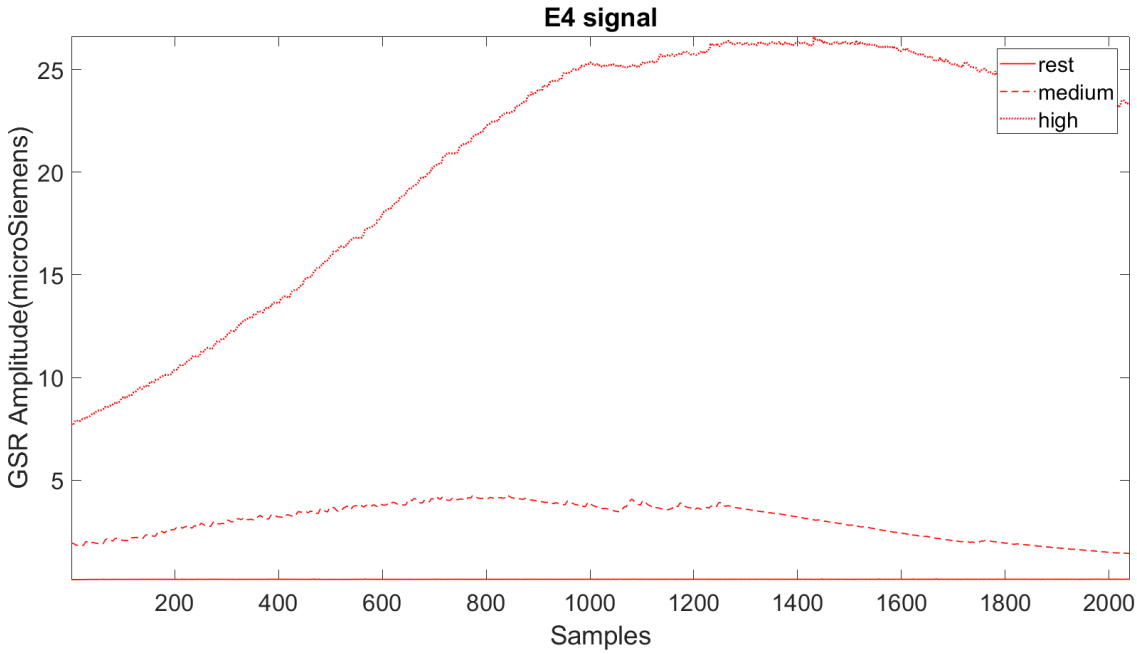


*Figure 5.8. Example of E4 signals relative to Subject 2.*

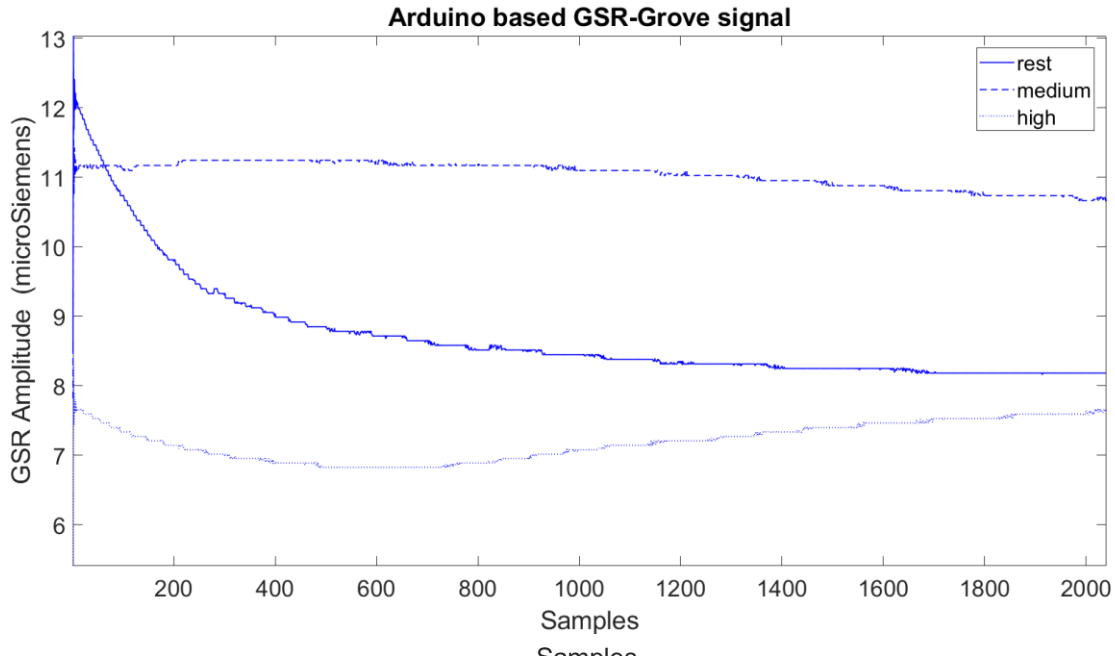


*Figure 5.9. Example of Arduino UNO based GSR-Grove signals relative to Subject 3.*

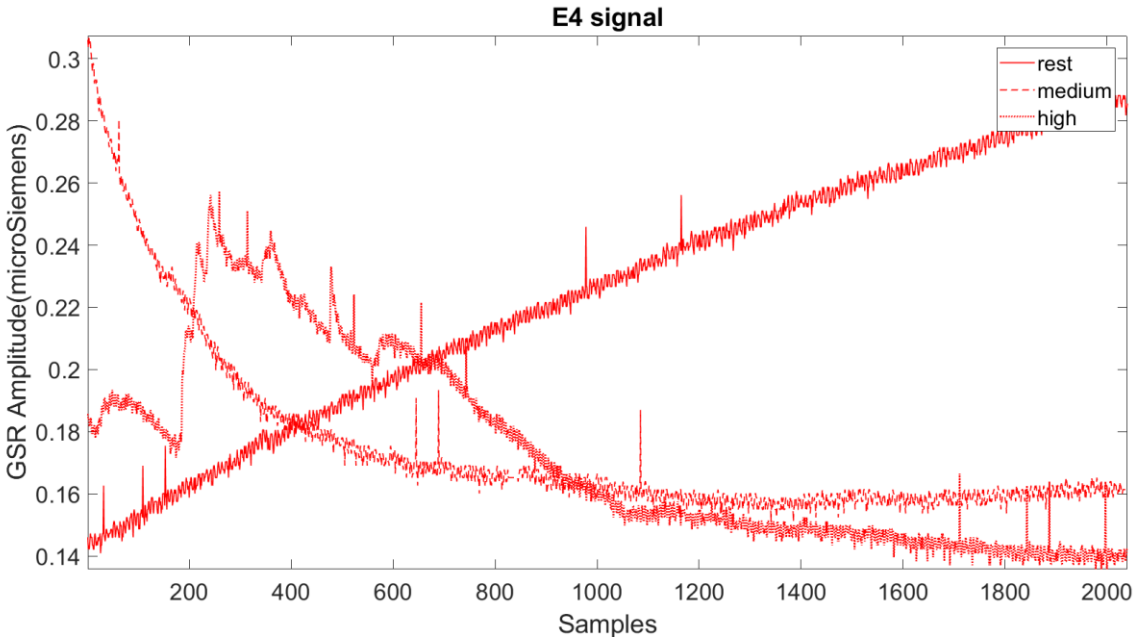


*Figure 5.10. Example of E4 signals relative to Subject 3.*

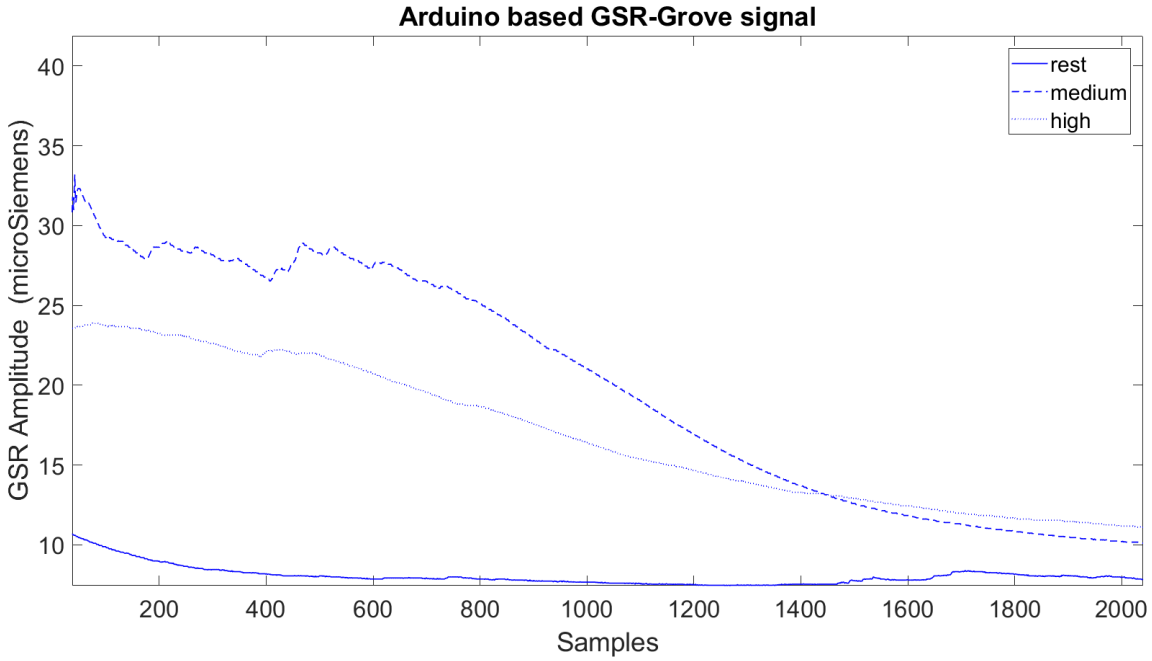


*Figure 5.11. Example of Arduino UNO based GSR-Grove signals relative to Subject 4.*

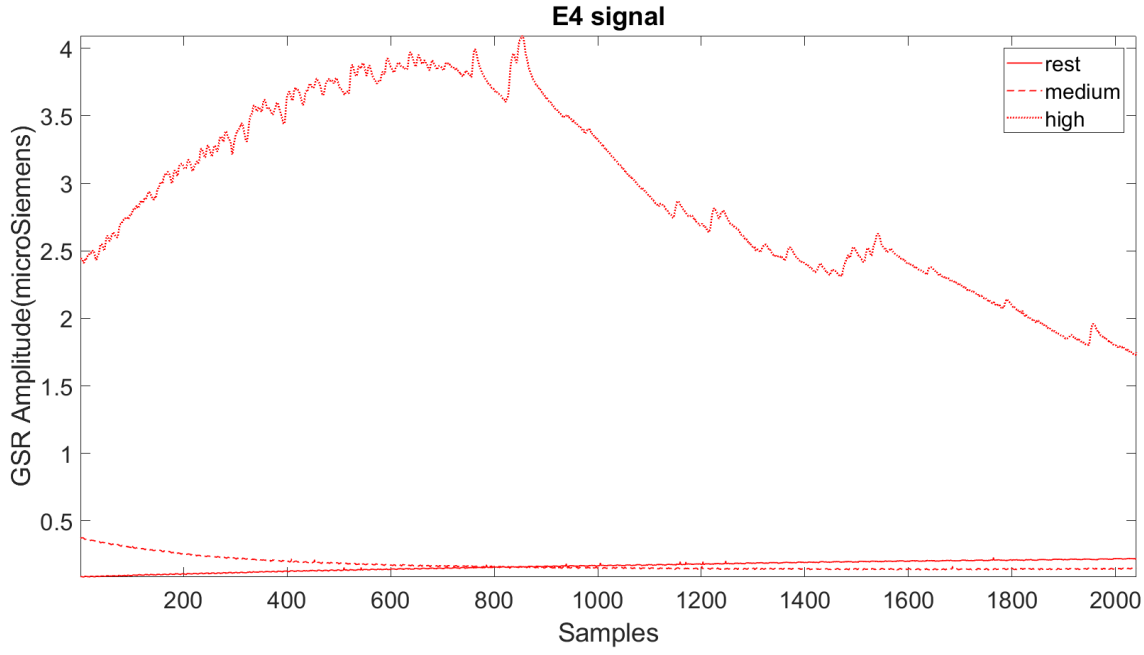


*Figure 5.12. Example of E4 signals relative to Subject 4.*

For each subject, two plots with signals of different colours are reported: Arduino UNO based GSR-Grove signals are represented in blue and E4 signals in red. The ordinate axis represents the signal amplitude in μS and the abscissa axis reports the number of samples. Moreover, each plot is provided with a legend to distinguish among the 3 different physical exercise levels. For each subject, the reported examples relative to a physical activity in the first plot corresponds to the simultaneously recorded signal relative to the same activity in the second plot. From these plots it is easy to understand the high variability that characterizes the GSR signal. This variability can be noticed on three different aspects: comparing Arduino UNO based GSR-Grove signals with E4 signals, comparing among different levels of physical activities and, finally, comparing subjects. In the first case, differences could be due to many factors related not only to the sensors, but also to the different recording sites [23]. In fact, range values of the two sensors are very different, but it is also difficult, by visual inspection, to find similarities across the signals recorded simultaneously [24]. Data recorded by using Empatica E4 shows lower and quite constant amplitudes after medium exercise or at rest than after high level of activity. This is true in Subjects 1,2 and 4, while for Subject 3 all the tracks seem to have similar ranges. Moreover, in the E4 signals relative to intense exercise there is a large presence of evident spikes in Subjects 1,3 and 4, while peaks are less evident in Subject 2, that, however, presents higher signal amplitude. These considerations can't be applied to Arduino UNO based GSR-Grove signals, where it is more difficult to a common trend for all the subjects. To support these considerations, the mean values of the signals have been computed. Specifically, for each subject, the corresponding average value of the signal' amplitude related to the same physical condition in the 3 sessions (i.e. Morning, Afternoon, Evening) was computed. Mean values are reported in *Table 5.2* and represented in *Figure 5.13.*

*Table 5.2. Dataset characteristics.*

| | **Arduino UNO based GSR-Grove mean GSR values (μS)** | | | **E4 mean GSR values (μS)** | | |
|---|---|---|---|---|---|---|
| | Rest | Medium | High | Rest | Medium | High |
| Subject 1 | 9,99 | 7,53 | 7,21 | 0,18 | 0,21 | 2,66 |
| Subject 2 | 12,27 | 16,08 | 20,24 | 0,16 | 2,44 | 15,91 |
| Subject 3 | 9,77 | 11,41 | 9,99 | 0,18 | 0,17 | 0,18 |
| Subject 4 | 10,61 | 12,89 | 12,60 | 0,17 | 0,19 | 1,31 |

From the mean values it is possible to confirm the high variability of data, that, in the case of Arduino UNO based GSR-Grove sensor, does not allow to find consistent considerations. In the case of the E4 sensor however, it is possible to observe that the mean values of the GRS signals increase with the increase of the exercise intensity, with exception of Subject 3, who maintains really low mean values for all the kinds of activity. Subject 2 reports the highest amplitudes also in the medium exercise intensity.

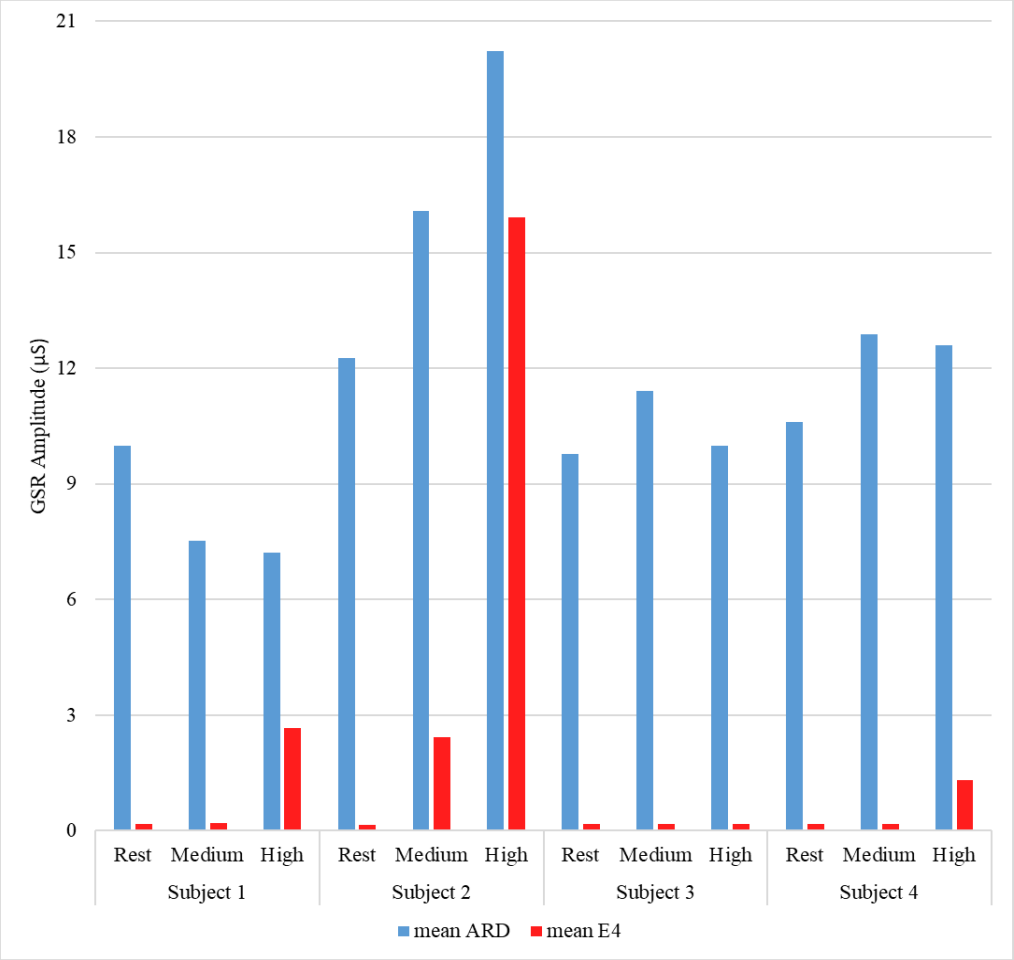


*Figure 5.13. Mean GSR amplitude for all subjects at different levels of physical effort.*

In the next sessions of this chapter, the results relative to the time domain analysis and frequency domain analysis after signal decomposition into tonic and phasic components will be presented. GSR signal decomposition has been performed in MATLAB with the implementation of a median filter based algorithm [7]. Then, for the frequency domain analysis the FFT magnitude of signals was computed using the *fft* function. These methodologies have been previously explained in Chapter 4.

## 5.1 Time domain analysis results

In the *Figures 5.14-5.19* some examples of the tonic and phasic components of the signals from different subjects, at different levels of physical effort are reported. These graphs are reported to have an initial representation of the time domain analysis results, that will be studied more in depth after the computation of the features.

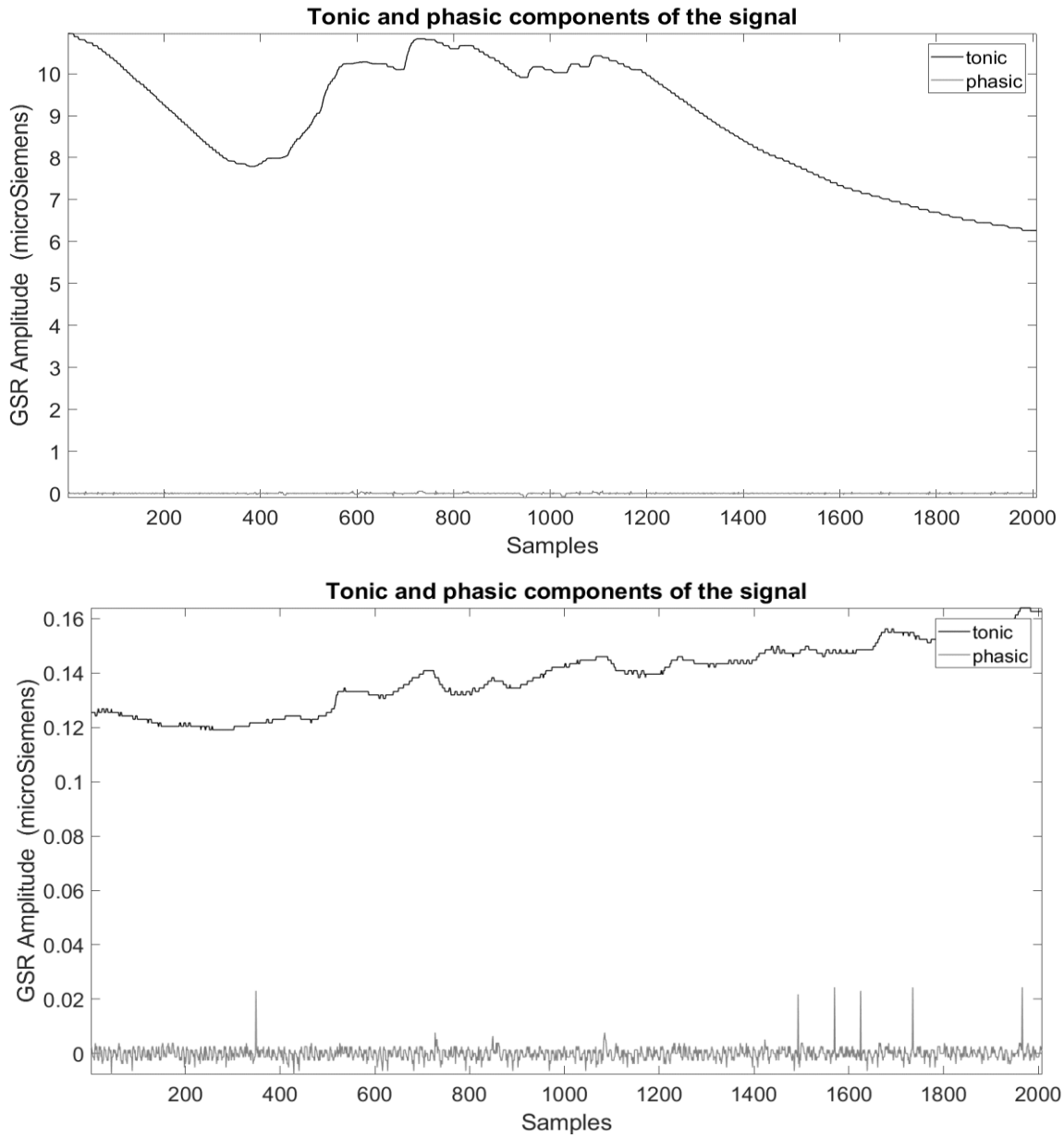


*Figure 5.14. Example of tonic and phasic components at rest relative to Arduino UNO based (upper panel) and E4 (lower panel) sensors of Subject 1.*

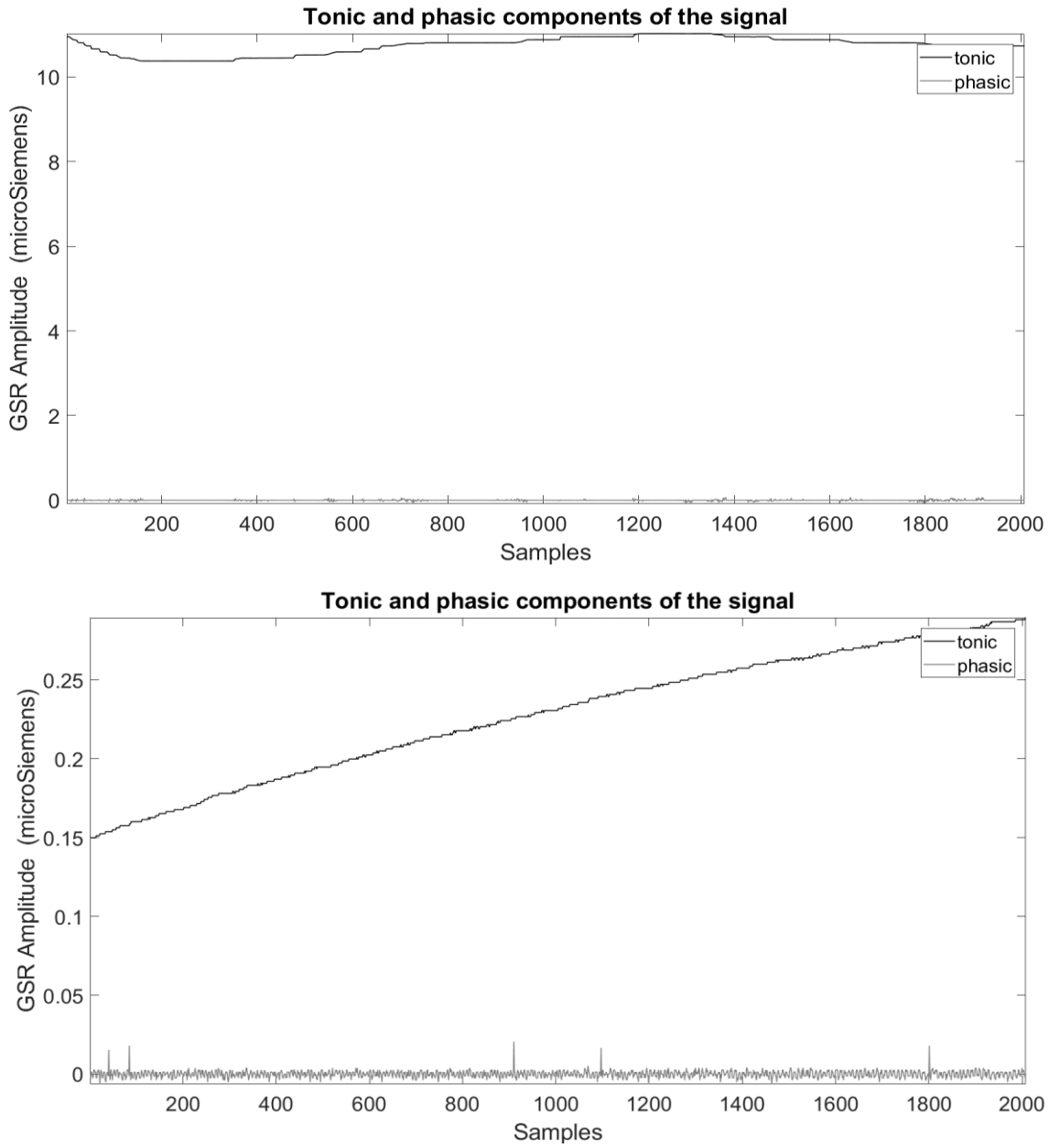


*Figure 5.15. Example of tonic and phasic components at rest relative to Arduino UNO based (upper panel) and E4 (lower panel) sensors of Subject 2.*

From a visual inspection, in *Figure 5.14* and *Figure 5.15*, relative to the sessions at rest, it is possible to see that there are differences among subjects in both the phasic and tonic components. The tonic component usually resembles the initial shape of the signal, before its decomposition. Similarities in the phasic component that belongs to the same sensors, the Arduino UNO based one or the E4 sensor, are recognizable. Phasic components are all zero-centred, while tonic components preserve the signal offset.

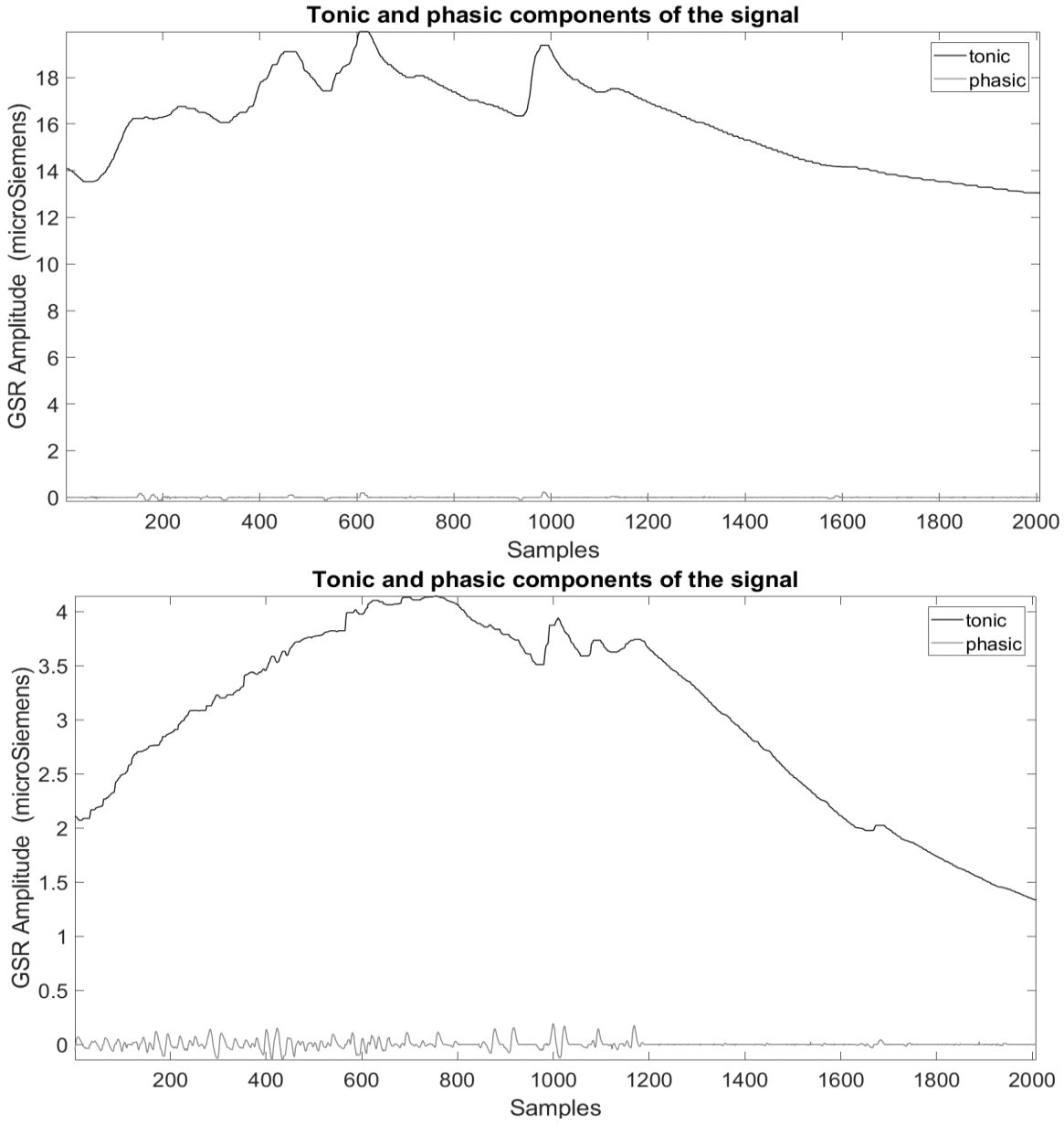


*Figure 5.16. Example of tonic and phasic components at medium exercise level relative to Arduino UNO based (upper panel) and E4 (lower panel) sensors of Subject 2.*

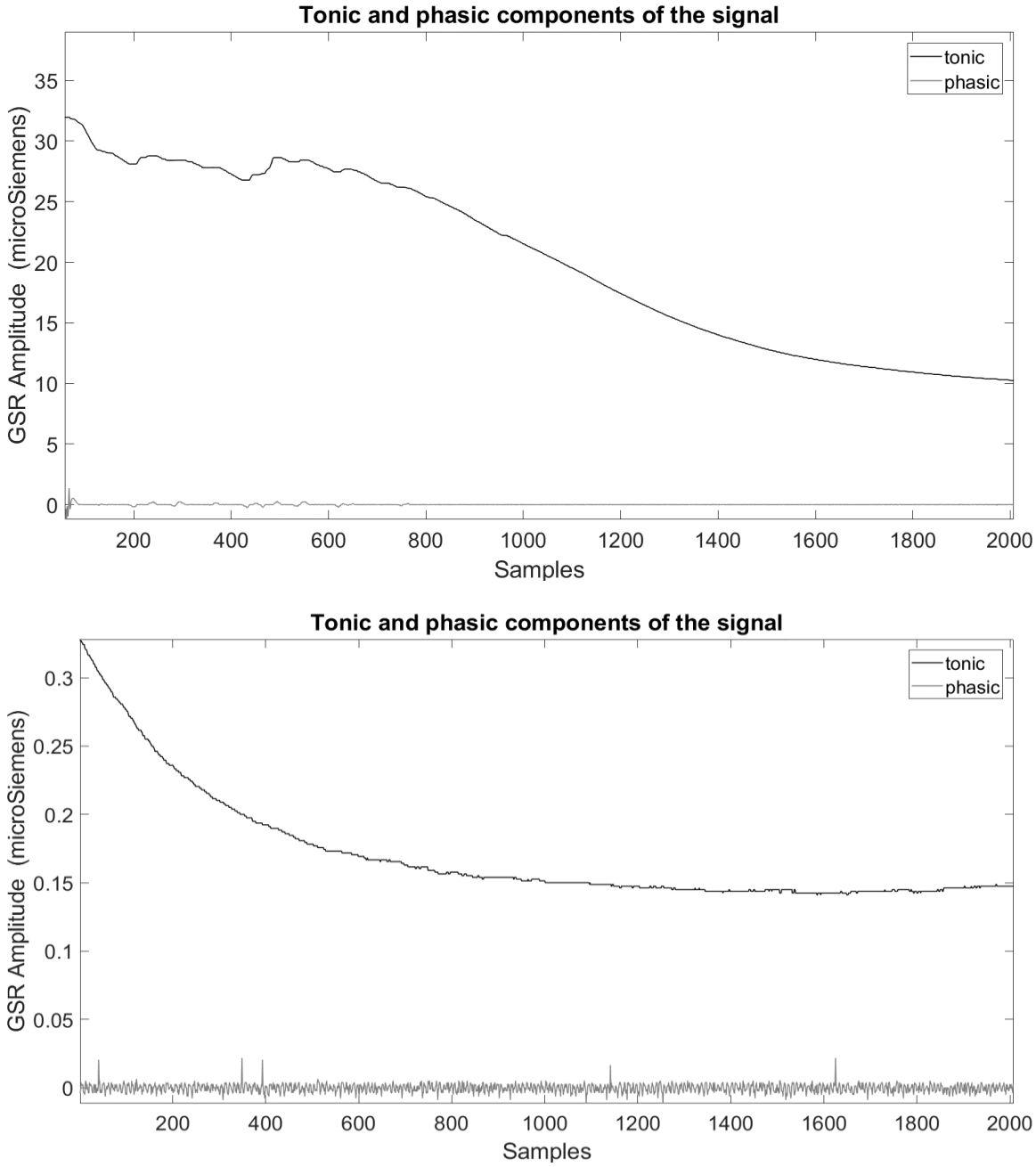


*Figure 5.17. Example of tonic and phasic components at medium level exercise relative to Arduino UNO based (upper panel) and E4 (lower panel) sensors of Subject 4.*

*Figure 5.16* and *Figure 5.17* represent two examples of the tonic and phasic components of signals recorded after a medium physical exercise. From these examples it is possible to observe how the response may vary among different subjects. Sometimes, both tonic and phasic components could present high responses, suggesting that the exercise performed with a medium intensity was able to elicit a large response. Subject 2 is an example of this

situation. In other cases, like for Subject 4, the response in the phasic component is less evident. However, both the selected subjects have in common the decreasing trend of the tonic component, resulting in a lower response in the last minutes of recording. This is particularly evident in Subject 4, relatively to the E4 sensor recording, where the tonic component has a decreasing trend that, at some point, reaches an almost constant behaviour. Also other signals recorded by using Empatica, and related to medium intensity exercises, show the same behaviour.

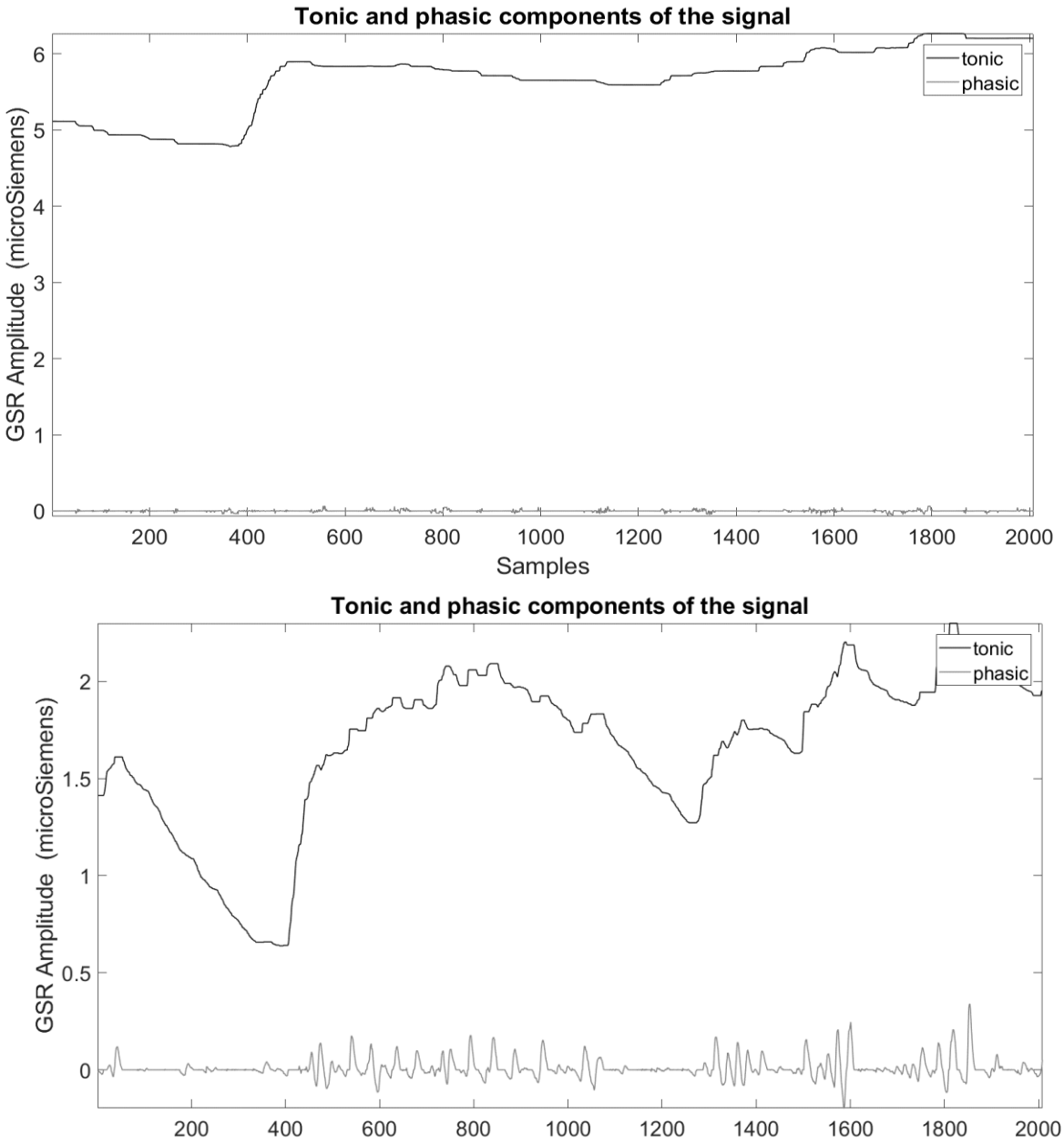


*Figure 5.18. Example of tonic and phasic components at high level exercise relative to Arduino UNO based (upper panel) and E4 (lower panel) sensors of Subject 1.*

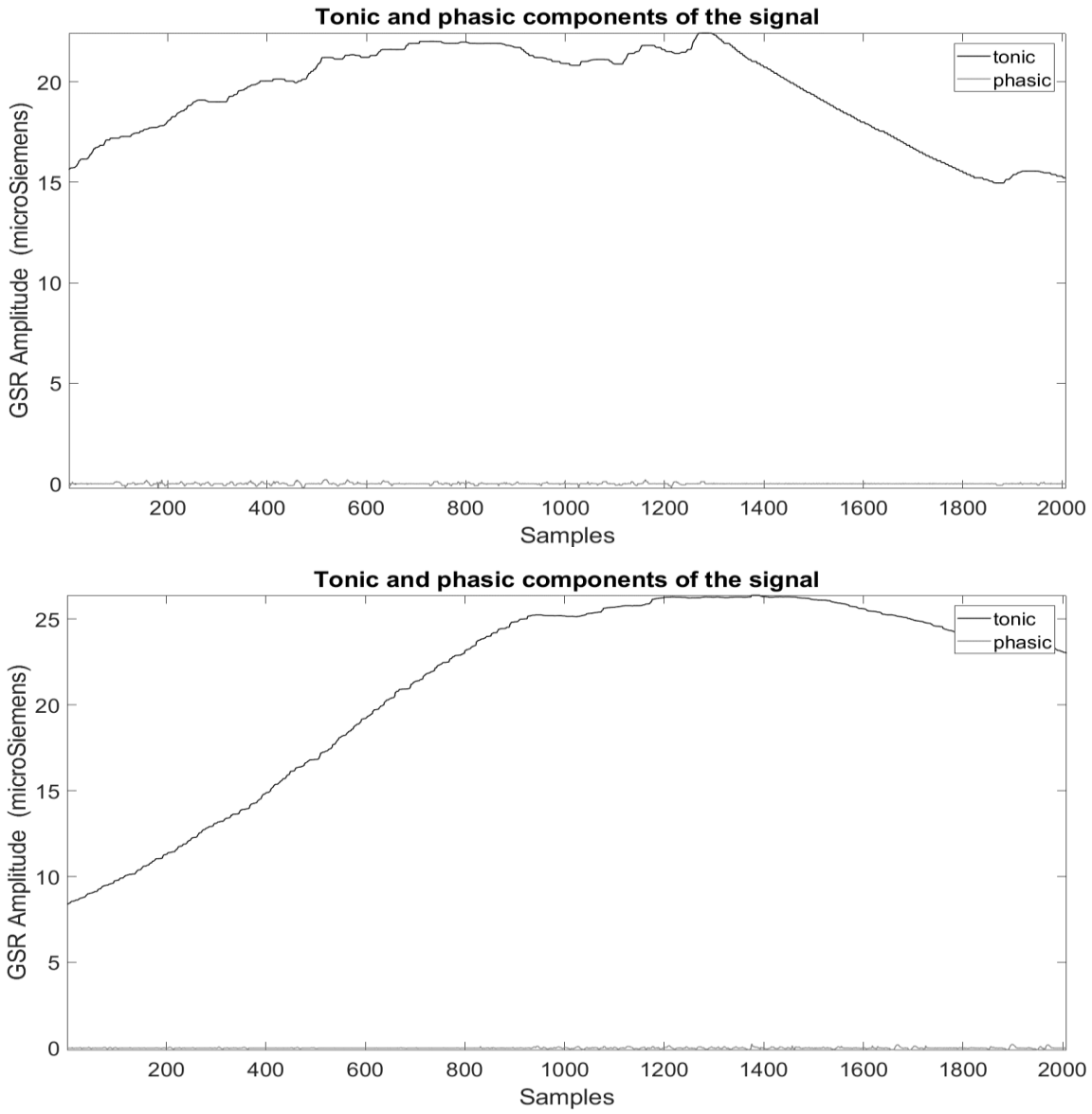


*Figure 5.19. Example of tonic and phasic components at high level exercise relative to Arduino UNO based (upper panel) and E4 (lower panel) sensors of Subject 2.*

In *Figure 5.18* an example of tonic and phasic components characterized by distinct SCR peak bursts of activations relative to the intense exercise recordings is reported. This kind of activation is observed in both the sensors, but it is more evident in the E4 one. *Figure 5.19* is a different example of response after intense exercise. It is evident that the tonic component reaches high values and that the activation increases at the beginning and lasts almost for the entire recording session. The phasic component presents peaks with higher amplitude in correspondence to the higher values of the tonic component.

### 5.1.1 Time domain features evaluation

In this section, the phasic and tonic components are compared by means of features computation. The features are extracted separately on each signal component, with the aim of finding which feature is more meaningful for the tonic and phasic component. The features with higher information content will be analysed to find which kind of information they are more prone to contain.

For each component of the signal, the features reported in Chapter 4 have been computed with a MATLAB code. For each level of activity, the features obtained from the 3 recording sessions (i.e. Morning, Afternoon, Evening) and related to the same subject and sensor have been averaged. To better evaluate the results given by the selected features, a data reduction protocol also explained in Chapter 4 was used. The discrepancy among the phasic and tonic components was computed using the normalised values of each feature, and only in the cases in which this variation was higher than 50% ($\Delta_{50\,\%}$) it was considered significant. All the variations among phasic and tonic components that were considered significant were used to fill in a table for every single feature. In each table, an "A" was reported if the significant variation was observed in the Arduino UNO based GSR-Grove sensor data, an "E" in the case the variation of at least 50% was observed in the E4 sensor measurements, and "A/E" if it was observed in both the sensors data. In tables' rows the subjects were reported, and the level of physical activity in the columns, to make, at the same time, comparisons on different aspects.

Tables representing the features computed in the time domain are listed below:

*Table 5.3*: Mean value

*Table 5.3. $\Delta_{50\,\%}$ for the mean value.*

| Subject/Activity | Rest | Medium | High |
|---|---|---|---|
| Subject 1 | / | / | E |
| Subject 2 | A | A | A/E |
| Subject 3 | / | A | / |
| Subject 4 | / | A | A |

*Table 5.4*: Area Under Curve

*Table 5.4. $\Delta_{50\,\%}$ for the AUC.*

| Subject/Activity | Rest | Medium | High |
|---|---|---|---|
| Subject 1 | / | / | E |
| Subject 2 | / | / | A |
| Subject 3 | / | / | / |
| Subject 4 | / | / | / |

*Table 5.5*: Standard Deviation

*Table 5.5. $\Delta_{50\,\%}$ for the STD.*

| Subject/Activity | Rest | Medium | High |
|---|---|---|---|
| Subject 1 | / | / | E |
| Subject 2 | / | / | / |
| Subject 3 | / | / | / |
| Subject 4 | / | / | A |

*Table 5.6*: Kurtosis

*Table 5.6. $\Delta_{50\,\%}$ for the Kurtosis.*

| Subject/Activity | Rest | Medium | High |
|---|---|---|---|
| Subject 1 | / | / | / |
| Subject 2 | / | / | / |
| Subject 3 | / | E | / |
| Subject 4 | A | / | E |

*Table 5.7*: Skewness

*Table 5.7. $\Delta_{50\,\%}$ for the Skewness.*

| Subject/Activity | Rest | Medium | High |
|---|---|---|---|
| Subject 1 | A/E | / | E |
| Subject 2 | E | E | E |
| Subject 3 | / | / | / |
| Subject 4 | A/E | / | / |

*Table 5.8*: Variance

*Table 5.8. $\Delta_{50\,\%}$ for the Variance.*

| Subject/Activity | Rest | Medium | High |
|---|---|---|---|
| Subject 1 | / | / | E |
| Subject 2 | / | / | E |
| Subject 3 | / | / | / |
| Subject 4 | / | A | A |

*Table 5.9*: Mean Derivative

*Table 5.9. $\Delta_{50\,\%}$ for the Mean Derivative.*

| Subject/Activity | Rest | Medium | High |
|---|---|---|---|
| Subject 1 | / | A | E |
| Subject 2 | / | / | / |
| Subject 3 | / | A | / |
| Subject 4 | / | A | A |

*Table 5.10*: Negative Mean Derivative

*Table 5.10. $\Delta_{50\,\%}$ for the Negative Mean Derivative.*

| Subject/Activity | Rest | Medium | High |
|---|---|---|---|
| Subject 1 | / | / | / |
| Subject 2 | / | / | / |
| Subject 3 | / | A | A |
| Subject 4 | / | / | / |

In the *Table 5.3* is possible to observe that the mean value feature results significative for the measurement data collected from both the sensors. To better understand differences among the tonic and phasic components, normalised values of the feature for all subjects, and related to the 3 levels of physical activity, are shown in *Figure 5.20*. Similar trends are also present in the AUC feature, but with less significance, so the bar graphs are not reported. The *Table 5.5* show STD significant differences only in Subject 1 and Subject 4, while, for

Subject 3, amplitudes are very low in both the components, and for Subject 2 differences are too small, as can be observed in *Figure 5.21*. Kurtosis feature does not result particularly significant, so it is not reported. Skewness feature variations principally involve the E4 sensor signals, indeed, as can be observed in the *Figure 5.22*, E4 values of this feature are all positive in the phasic component. Similarly to STD, the variance significance is more related to the different subjects, involving E4 sensor in Subjects 1 and 2, and Arduino UNO based GSR-Grove in Subject 4. Mean Derivative and Mean Negative Derivative features are relevant only for the Arduino UNO based GSR-Grove sensor, suggesting that in the E4 recorded signals this information does not allow to distinguish between the phasic and tonic components. However, even if there are important changes in the other sensor, the Arduino UNO based one, it is difficult to associate these changes to any relation among subjects or physical activity and, for this reason, comparison graphs are not reported.

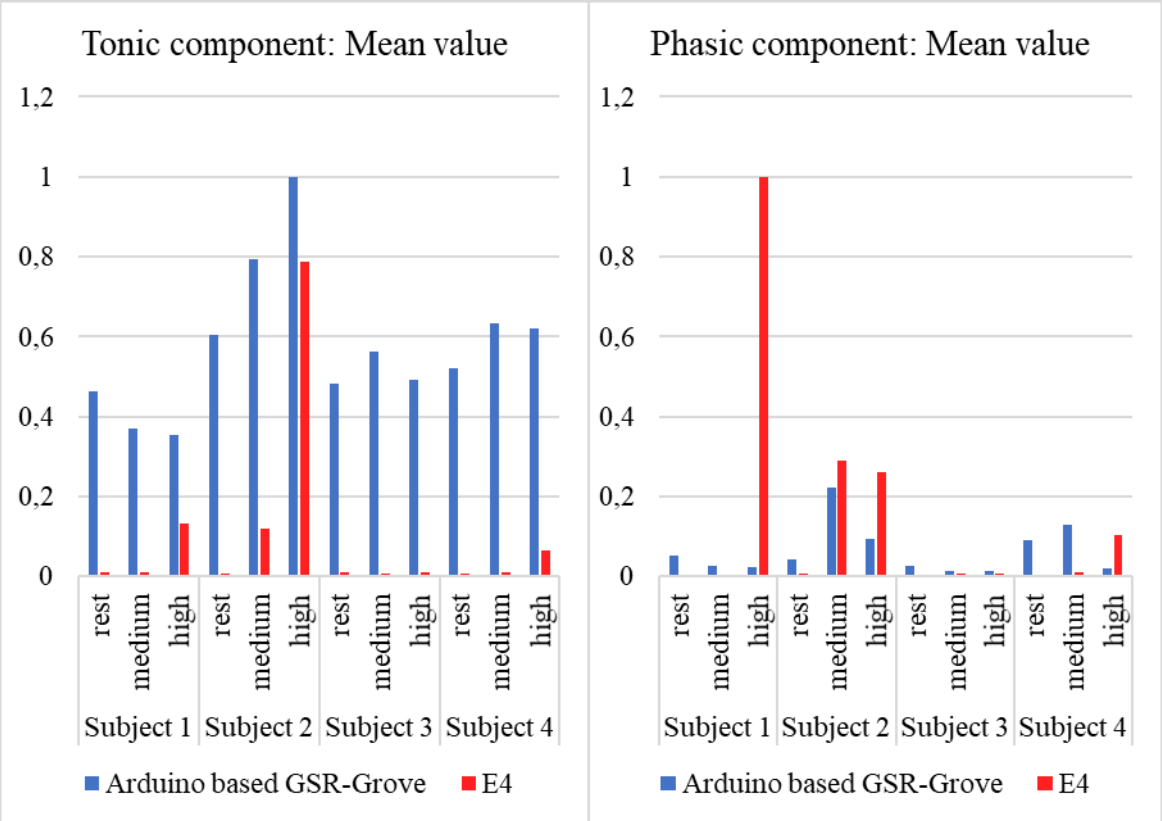


*Figure 5.20. Comparison among normalised mean values of tonic (left) and phasic (right) components for all the subjects in the 3 physical activity conditions.*

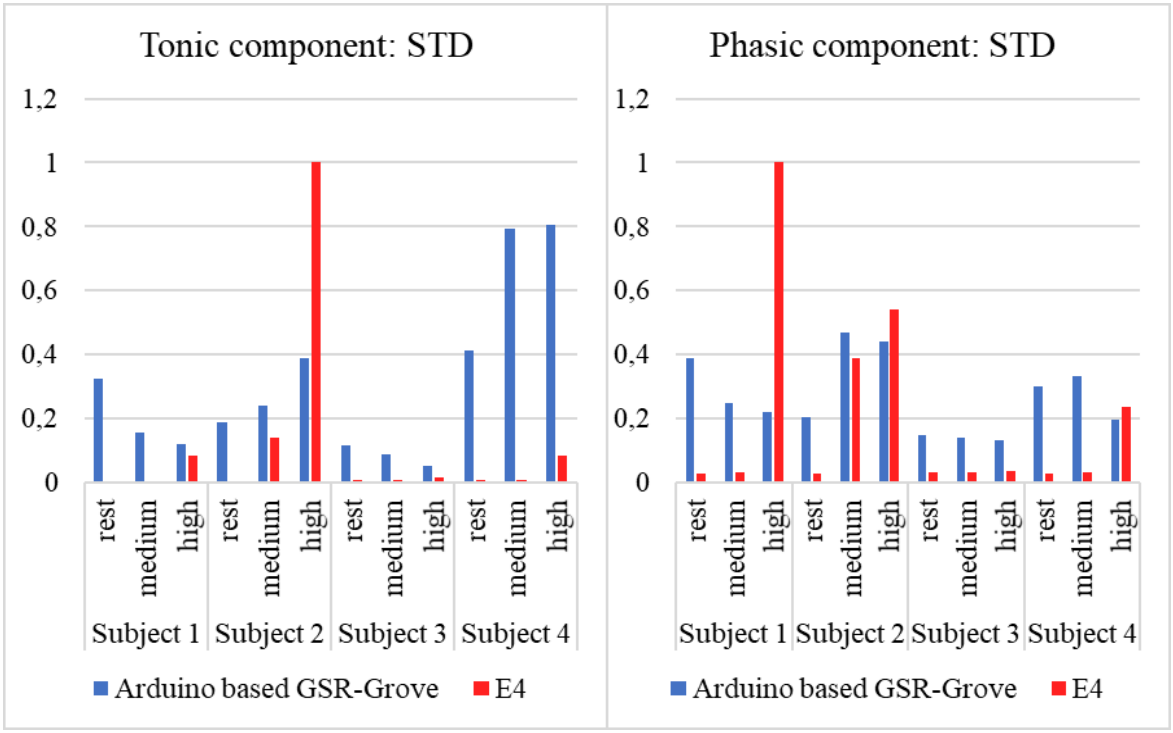


*Figure 5.21. Comparison among normalised STD values of tonic (left) and phasic (right) components for all the subjects in the 3 physical activity conditions.*

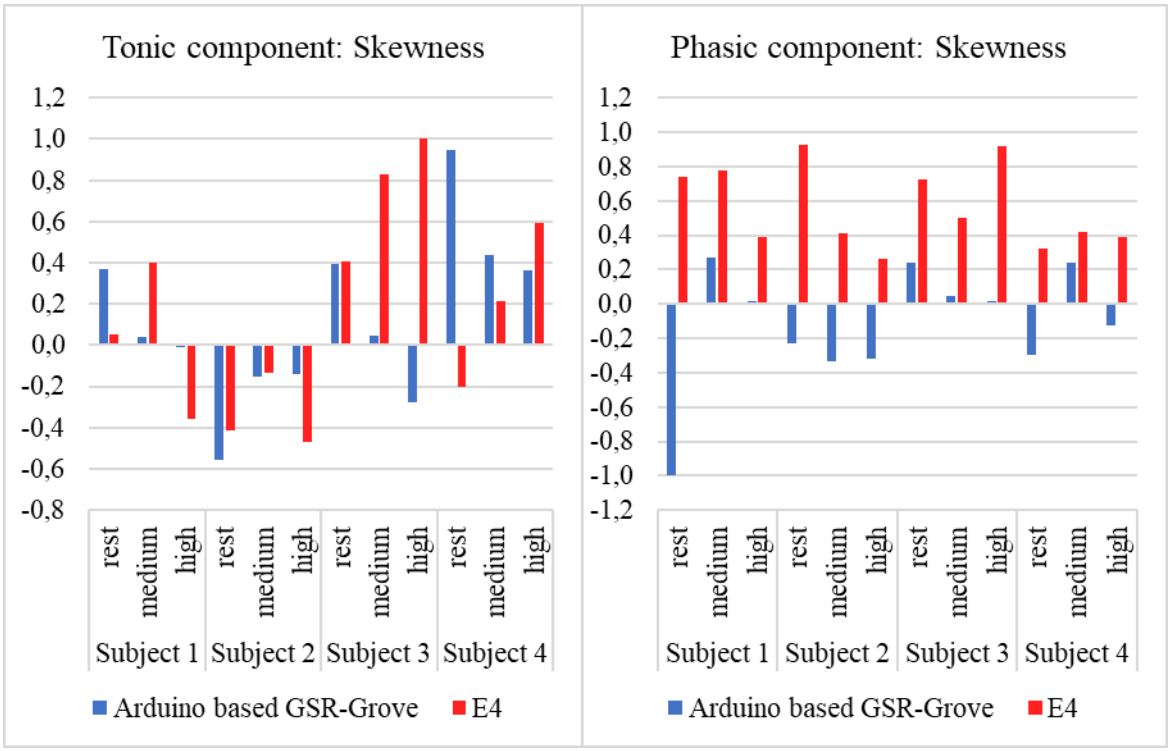


*Figure 5.22. Comparison among normalised STD values of tonic (left) and phasic (right) components for all the subjects in the 3 physical activity conditions.*

## 5.2 Frequency domain analysis results

As reported in Chapter 4, in the session relative to the frequency analysis, FFT magnitude values of both the tonic and phasic components have been computed in MATLAB. In the *Figures 5.23-5.25*, some examples of the FFT magnitude of tonic and phasic components are reported in dB, while in the abscissa axis are reported the corresponding frequencies in Hz.

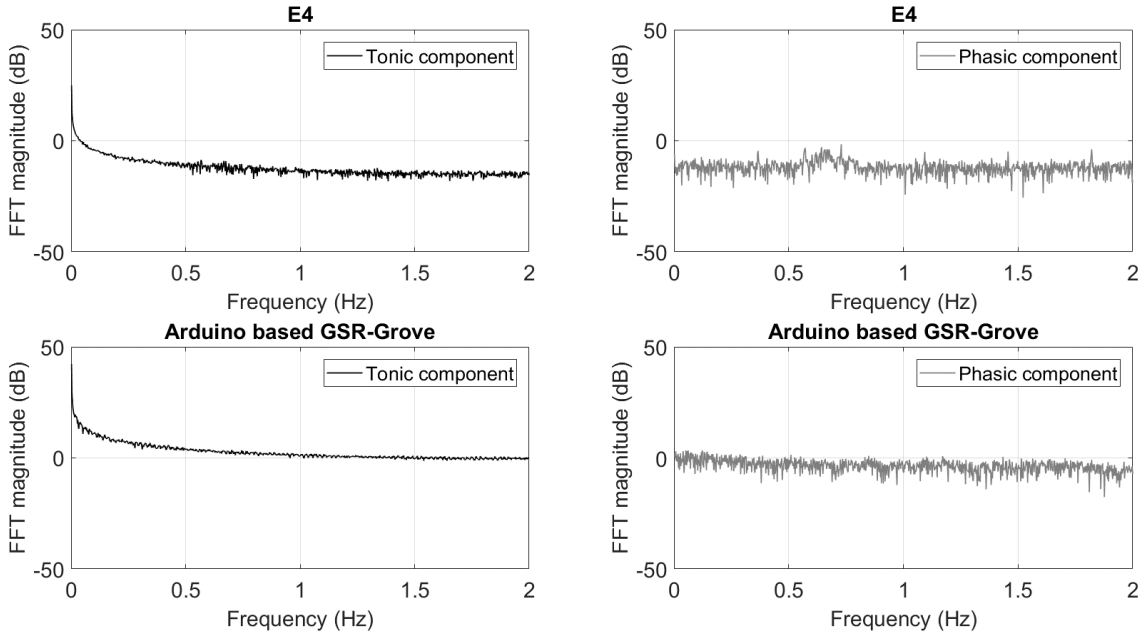


*Figure 5.23. FFT magnitude of the tonic and phasic components at rest condition for Subject 2.*

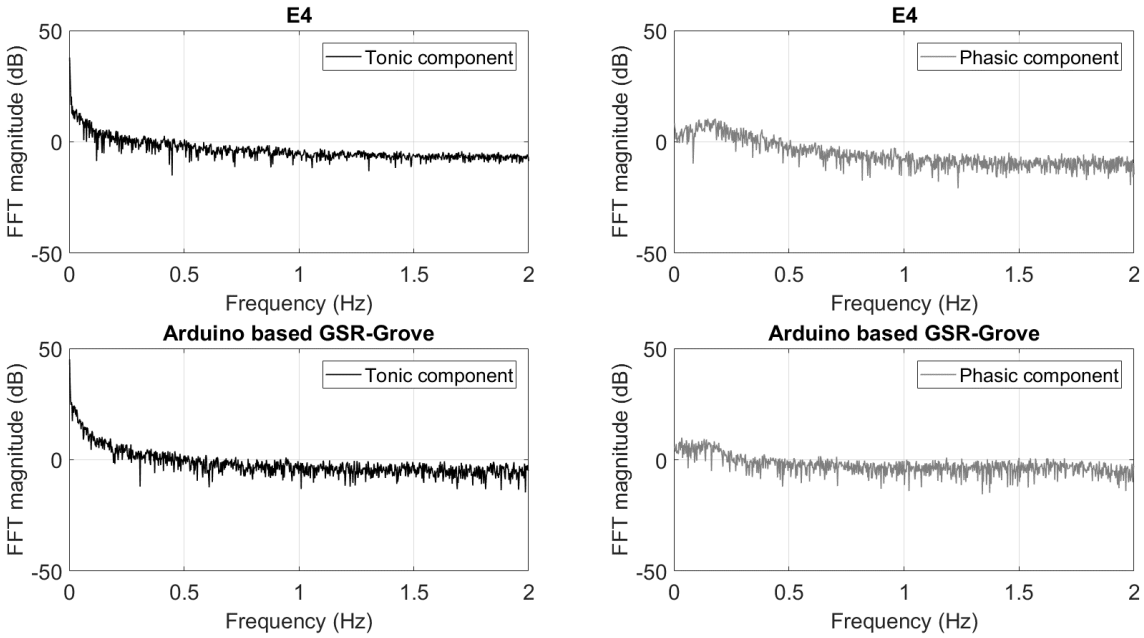


*Figure 5.24. FFT magnitude of the tonic and phasic components at medium activity for Subject 2.*

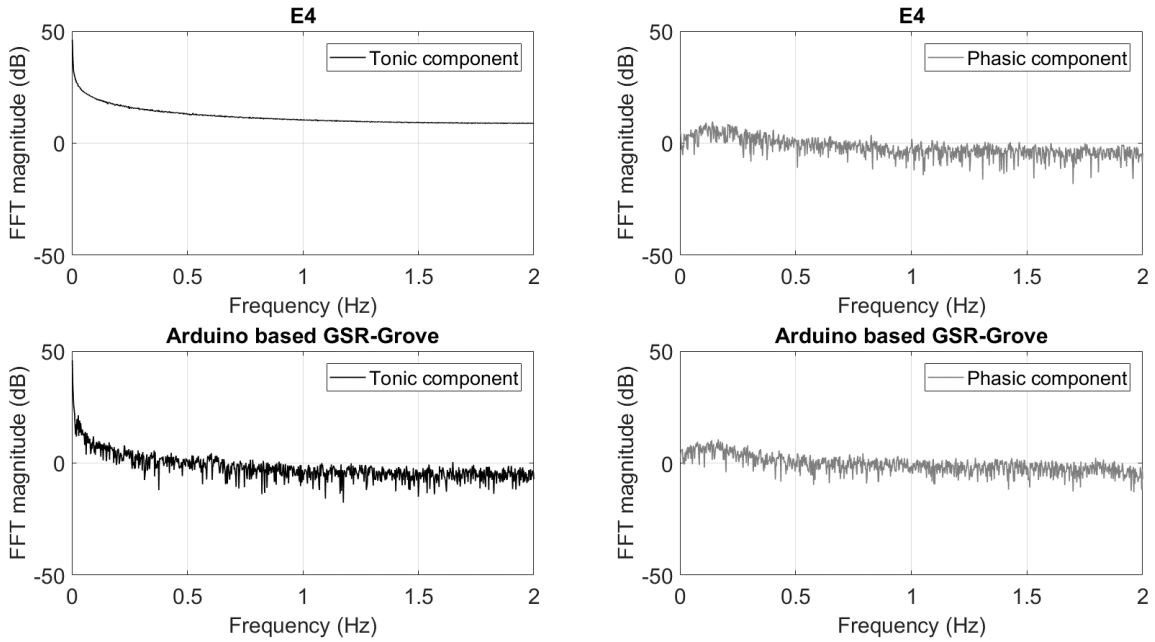


*Figure 5.25. FFT magnitude of the tonic and phasic components at high activity for Subject 2.*

From the *Figures 5.23-5.25* it is possible to observe differences between the FFT magnitude of the tonic components, reported on the left side of the figures, and that of the phasic component, on the right side. FFT magnitude of Subject 2 is reported in three examples, one for each different physical activity condition, for the E4 sensor (upper part of the figures) and the Arduino UNO based GSR-Grove sensor (lower part of the figures). The FFT magnitude of the tonic component has maximum values corresponding to the lower frequencies and decreases with the increase of the frequency. The FFT magnitude of the phasic component, instead, has maximum values at higher frequencies than those of the tonic component. In particular, looking at both medium and high intensity exercise levels, the maximum values of the phasic components are observed in the frequency band [0-0.5] Hz [17], while, for the condition at rest, this similarity does not occur across the different Subjects.

### 5.2.1 Frequency domain features evaluation

In this section, unlike what was done in paragraph 5.1.1, the phasic and tonic components are compared using the features computed in the frequency domain, on the FFT magnitude signals. The features are calculated separately on each component of the FFT magnitude signal to find which feature is capable of discriminating the information content of the signal between the tonic and the phasic component.

The features computed in the frequency domain are listed in Chapter 4, where it is also explained how the tables related to the information content of each feature were filled in, to reduce the amount of data to analyse. As previously done for the time domain, the tables showing deltas with a variation greater than 50% are also proposed in this context.

Tables representing the features computed in the frequency domain are listed below:

*Table 5.11*: Mean value of FFT magnitude

*Table 5.11.* $\Delta_{50\,\%}$ *for the mean value of FFT magnitude.*

| Subject/Activity | Rest | Medium | High |
|---|---|---|---|
| Subject 1 | A | / | / |
| Subject 2 | A | / | E |
| Subject 3 | / | / | / |
| Subject 4 | A | A | A |

*Table 5.12*: Signal Magnitude Area

*Table 5.12.* $\Delta_{50\,\%}$ *for the SMA.*

| Subject/Activity | Rest | Medium | High |
|---|---|---|---|
| Subject 1 | / | / | / |
| Subject 2 | / | / | / |
| Subject 3 | / | / | / |
| Subject 4 | / | / | / |

*Table 5.13*: Standard Deviation

*Table 5.13. $\Delta_{50\,\%}$ for the STD.*

| Subject/Activity | Rest | Medium | High |
|---|---|---|---|
| Subject 1 | / | / | / |
| Subject 2 | / | / | / |
| Subject 3 | / | / | / |
| Subject 4 | / | / | / |

*Table 5.14*: Kurtosis

*Table 5.14. $\Delta_{50\,\%}$ for the Kurtosis.*

| Subject/Activity | Rest | Medium | High |
|---|---|---|---|
| Subject 1 | / | / | / |
| Subject 2 | / | / | / |
| Subject 3 | / | / | / |
| Subject 4 | / | / | / |

*Table 5.15*: Skewness

*Table 5.15. $\Delta_{50\,\%}$ for the Skewness.*

| Subject/Activity | Rest | Medium | High |
|---|---|---|---|
| Subject 1 | A/E | A/E | A |
| Subject 2 | A/E | A | A/E |
| Subject 3 | A/E | A/E | A/E |
| Subject 4 | A/E | A/E | A/E |

*Table 5.16*: Range

*Table 5.16. $\Delta_{50\,\%}$ for the Range.*

| Subject/Activity | Rest | Medium | High |
|---|---|---|---|
| Subject 1 | / | / | / |
| Subject 2 | / | / | / |
| Subject 3 | / | / | / |
| Subject 4 | / | / | / |

*Table 5.17*: Energy

*Table 5.17.* $\Delta_{50\,\%}$ *for the Energy.*

| Subject/Activity | Rest | Medium | High |
|---|---|---|---|
| Subject 1 | / | / | E |
| Subject 2 | / | / | A |
| Subject 3 | / | / | / |
| Subject 4 | / | / | / |

*Table 5.18*: Entropy

*Table 5.18.* $\Delta_{50\,\%}$ *for the Entropy.*

| Subject/Activity | Rest | Medium | High |
|---|---|---|---|
| Subject 1 | A/E | A/E | A/E |
| Subject 2 | A/E | A | A |
| Subject 3 | A/E | A/E | A |
| Subject 4 | A/E | E | / |

In *Table 5.11* it is possible to observe that the mean FFT magnitude results significant for Subject 2 and Subject 4. To have deeper information about differences among the tonic and phasic components, the normalised values of the feature under observation are shown in *Figure 5.26*. The Figure shows that for Subject number 2 there is a variation in the value relative to the high intensity exercise, from positive to negative, looking firstly at the tonic component and then at the phasic one, of the E4 sensor measurements bars. The same occurs for Subject 4 in the Arduino UNO based sensor measurements, at all the activity levels. These results suggest that E4 sensor is sensitive to changes in the tonic component in Subject 2, that increase with the increase of activity, while Arduino UNO based sensor reports high values of tonic component in Subject 4 and low values in the phasic component. The *Table 5.15* shows that regarding Skewness of the FFT magnitude there are significant differences in all the subjects and for both sensors. In *Figure 5.27* the tonic component presents high values, but what is of interest is that in the phasic component there are important changes among different exercise levels. In particular, except for Subject 3, in both the sensors'

measurements it is possible to see that with the increase of exercise intensity, the Skewness becomes less negative (or more positive). In *Table 5.17* significant differences are observed only in the case of high intensity exercise. Data relative to this feature are reported in *Figure 5.28*. In the phasic component there is an increase in energy with the increase of the activity level, except in Subject 3, where values are also quite small, and in the Arduino UNO based sensor measurement values of Subject 4. Considering the tonic component part of the graph, it is interesting to observe the values of Subject 2, that, especially for the E4 sensor, increase with the activity. Last Table to comment is *Table 5.18*, where results are significant for both sensors across all the subjects. In *Figure 5.29*, the phasic component, on the right, achieves high values of Entropy for all the subjects. An interesting observation that can be made on the tonic component for the E4 sensor values is that the Entropy increases with the increase of the level of activity. This information could be useful to discriminate among the different levels of activity. For what concerns the other frequency features, significant differences have not been highlighted, as shown in the relative tables, so the bar graphs are not reported.

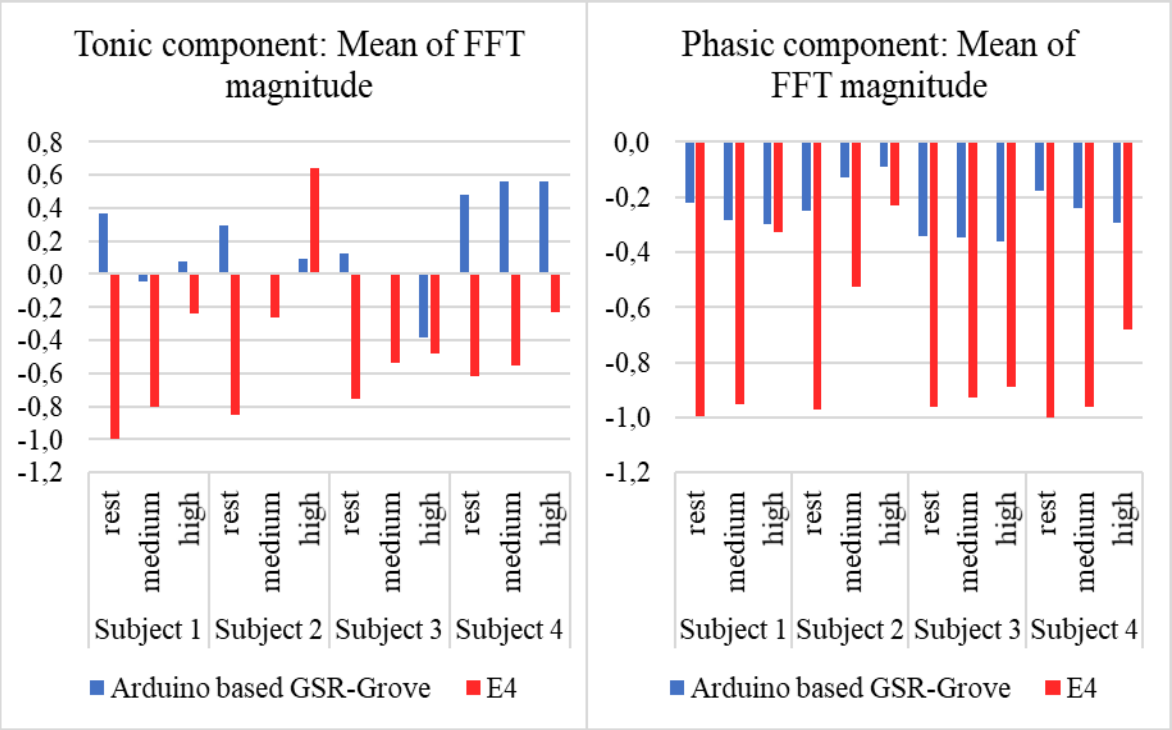


*Figure 5.26. Comparison among normalised mean FFT magnitude values of tonic (left) and phasic (right) components for all the subjects in the 3 physical activity conditions.*

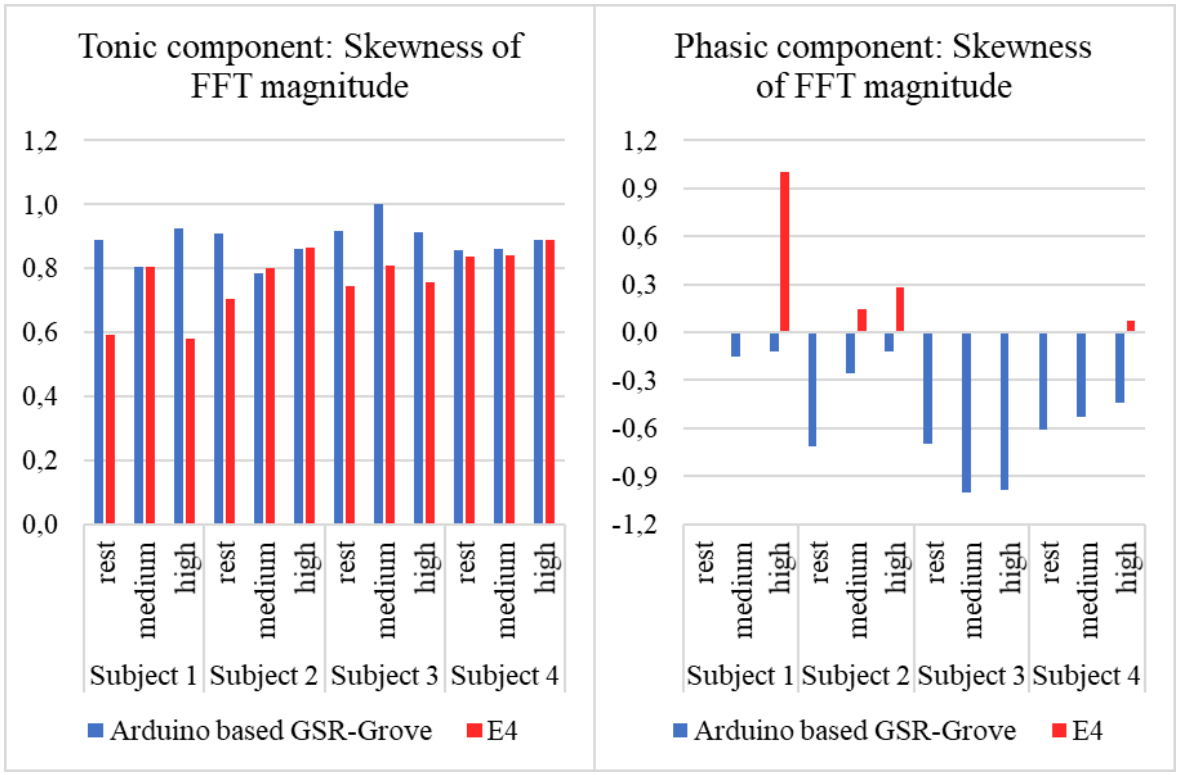


*Figure 5.27. Comparison among normalised Skewness values of tonic (left) and phasic (right) components for all the subjects in the 3 physical activity conditions.*

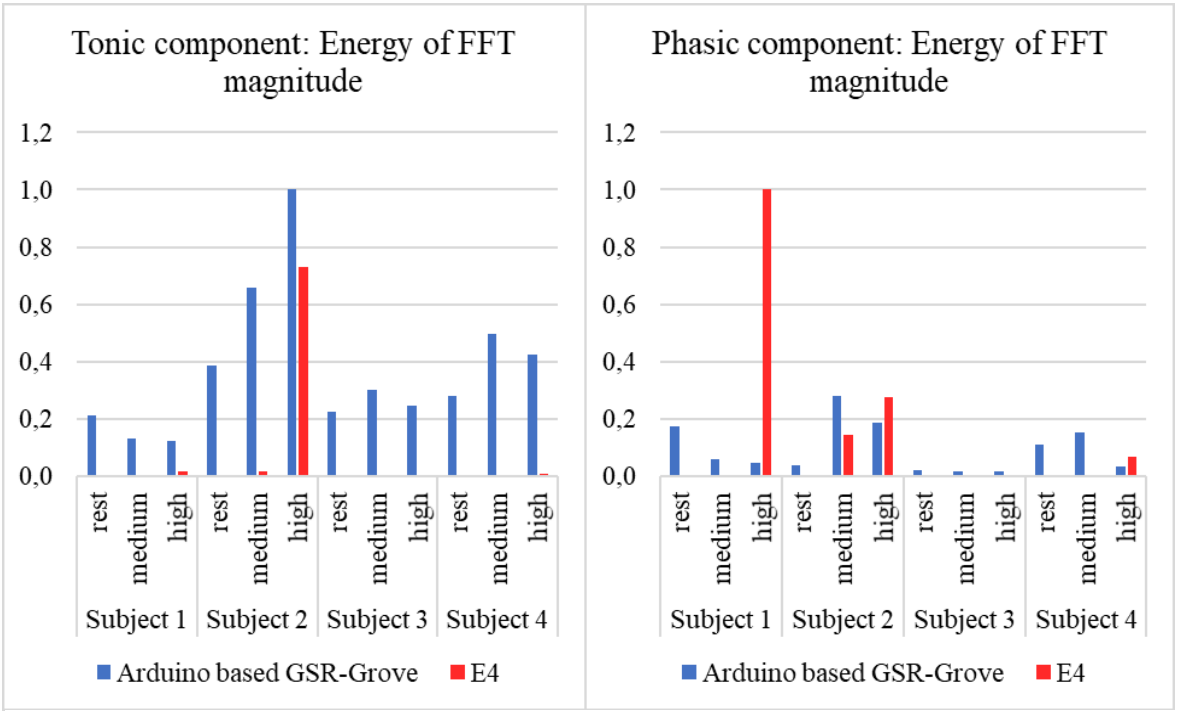


*Figure 5.28. Comparison among normalised Energy values of tonic (left) and phasic (right) components for all the subjects in the 3 physical activity conditions.*

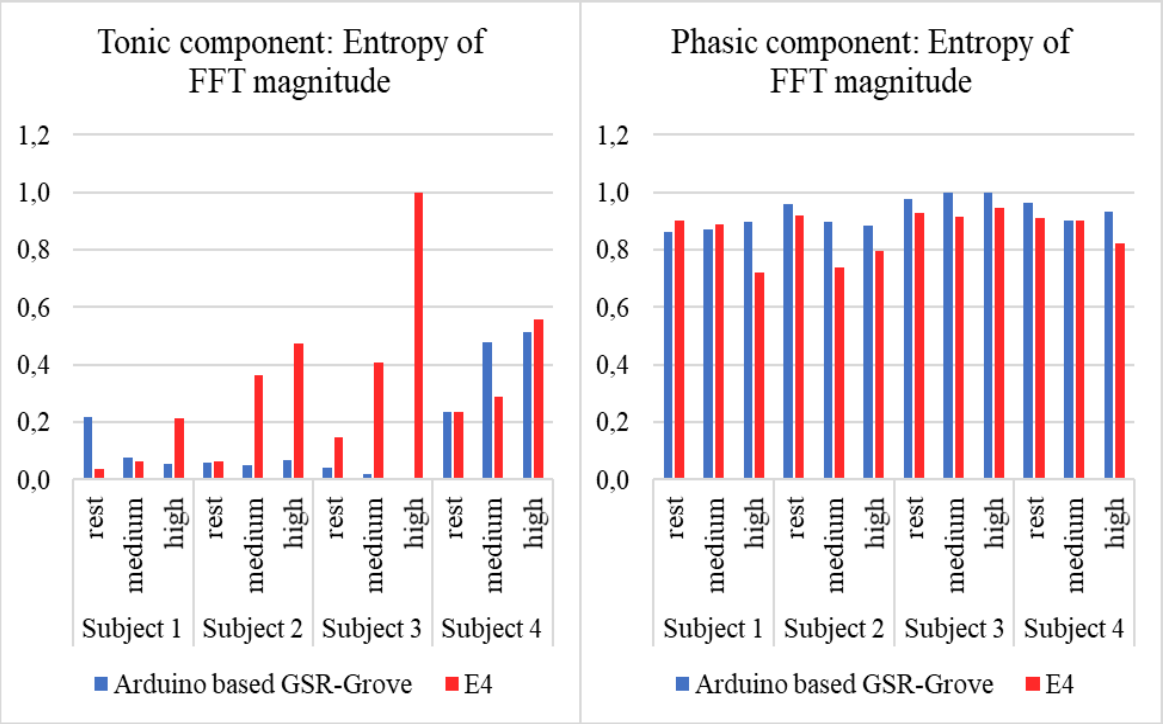


*Figure 5.29. Comparison among normalised Entropy values of tonic (left) and phasic (right) components for all the subjects in the 3 physical activity conditions.*

n the next Chapter, all the presented results will be discussed to underline the outcomes of the entire experiment and to provide final considerations.

# Chapter 6

# Discussion and Conclusion

From a first look to the initial part of the results, it is evident that the GSR signal is characterised by a great variability. The most important information that emerges from the experiments is that, for the E4 sensor, both considering the qualitative MATLAB plots and the mean GSR amplitude of the signals, there is an increase in the total signal response with the increase of the level of the performed physical activity [17]. For the Arduino UNO based GSR-Grove sensor, instead, the same consideration does not hold for all the subjects. Analysing each different subject, it appears that, when exposed to physical activity, there are principally two different kinds of response, especially looking at the signals measured by the E4 sensor: in Subjects 1, 3 and 4 the presence of distinct SCR peak bursts can be evidenced, while, in Subject 2, at high level of physical activity there is a greater increase in the signal amplitude values, with respect to the other subjects. This could be due to the physiological characteristics of the subject, or to the different perception, among subjects, of the same exercise intensity. Moreover, it was possible to observe that Subject 3, a 59-year-old woman, is the one who presents less variations in the GSR mean amplitude recorded with the E4 sensor. By applying the algorithm presented in [7]. GSR measurement data was decomposed into its two main components, the tonic and the phasic one. This step was performed in order to find the characteristics that mainly differentiate these two components, and to better understand their information content. The analysis was carried out both in the time domain and in the frequency domain, by visual inspection of the signals and by the computation of some features that are, in the literature, the ones most frequently selected for the GRS signal [8][19]. In most studies aimed at the classification of EDA signals, no preliminary feature selection is usually implemented, or this is done automatically by the classifier, without taking into account pattern recognition algorithms related to the target to be identified [8]. This work, therefore, is focused on trying to identify which features are more significant for one signal component rather than another, which are more significant for a certain subject or sensor, and which are not very informative for this kind of experiment. Considering the use of classifiers for the discrimination of the level of physical activity carried out by a

certain person, these considerations could be used to attribute proper weights to the features, avoiding these weights to be chosen automatically by the classifier, and not based on the information content. From the time domain analysis, it was possible to observe that the phasic component, which is zero centred, corresponds to high frequencies information, while the tonic component resembles most the slowly varying component of the original signal, maintaining a variable offset. Thanks to the decomposition of the signal, it was possible to attribute the different behaviour observed in Subject 2, when undergoing intense effort, to the tonic component. On the other hand, the presence of distinct SCR peak bursts in the other subjects is recognizable in the morphology of the phasic component. Regarding the feature analysis in time domain, results shown relevant significance mainly in three features, out of the eight computed on the signals: Mean value, STD and Skewness. The Mean value, computed on the measurements performed with the E4 sensor, confirms that with the increase of the exercise intensity, there is an increase in both the signal components, compared to the rest condition. In Subject 2, especially the tonic component shown a consistent increase. For the measurements performed with the Arduino UNO based sensor, this feature has a relevant value in the tonic component, but it is not helpful in the discrimination of the exercise level. For the STD feature, an increase of its value appears with the increase of the activity intensity, for the measurements collected with the E4 sensor, and differences across subjects are found, about how the information between tonic and phasic components is distributed. In the measurements performed with the Arduino UNO based sensor on Subject 3, there was a significant variation in the tonic component at high intensity exercise, maybe suggesting that for this subject the signal recorded from the fingerprints gave high response. Skewness of the E4 sensor signal measurements reported all positive values in the phasic component, which means that there is a greater number of samples that tend to have a higher value than the average one. This is useful to differentiate the tonic component from the phasic one, but it does not give any further information. AUC feature confirmed what already stated for the Mean value, and Variance confirmed STD outcomes, but both with less significance. For what concerns the frequency domain analysis, features were computed on the FFT magnitude of the separated phasic and tonic components [25]. From the MATLAB plots scaled in dB, it was possible to observe that the frequency band [0-0.5] Hz contains the most information and that the tonic component corresponds to very low frequencies, while the phasic component is related to a higher frequency content

[17] [26] [27]. Frequency domain analysis shown relevant significance mainly in four features, out of the eight computed on the signals: Mean value of FFT magnitude, Skewness, Energy and Entropy. For the measurements collected with the Arduino UNO based sensor, the Mean value of FFT magnitude shown significance for Subject 4, confirming that its tonic component has higher response with respect to other subjects. For the measurements performed with the E4 sensor, the mean FFT magnitude becomes less negative with the increase of the activity intensity, for all the subjects and in both the signal components, so this feature could be helpful in classifying the different levels of physical effort. Skewness feature shown great differences in all subjects for both sensors. This feature is sensitive to variations in the phasic component, that, for the E4 sensor measurements becomes less negative with the increase of the activity intensity, and the same happens for Arduino UNO based sensor measurements, for Subject 2 and Subject 4. The Energy feature reported differences in the energy distribution among subjects. In the phasic component, the Energy increased with exercise intensity. Subject 2 shown high energy increase also in the tonic component. Entropy, instead, was more variable in the tonic component, where, for the E4 sensor measurements, it increased with the activity level. Changes in this feature are completely related to the tonic component [28].

Focusing on the two measurement devices, E4 wristband and the Arduino UNO based GSR-Grove sensor, significant differences were encountered [29]. In the E4 sensor measurements, results were more consistent across all the subjects and it was easier to relate signal behaviour to the changes in the physical activity, while for the Arduino UNO based sensor measurements, significant differences were found between phasic and tonic components, but it was more difficult to relate these results to the change in the exercise intensity [30]. From the signal decomposition point of view, some other considerations can be done at this point of the work, that could be helpful for the interpretation of the results. In fact, the analysis of GSR signals in the time domain provides a lot of physiological information, that are subject-dependent because they are related to the variability of the response of each subject to the same stimuli. These differences in the signal behaviour can be due to intrinsic physiological characteristics of the subject, like gender, age and sweat glands density in the different locations of the body, and to extrinsic physiological characteristics, such as the level of physical training and fitness conditions of the subject, which brings to a different perception on the effort requested to perform the physical activity. These aspects could be reflected in

the computed features and could be used to implement subject-dependent classification algorithms, to consider user-related characteristics [31]. On the other hand, frequency domain analysis demonstrated significance in the discrimination of different levels of activities and in the attribution of this differences to a signal component rather than another.

To conclude, the E4 wrist-worn device results to be superior to the Arduino UNO based GSR-Grove sensor, for the many reasons discussed above, together with the fact that it is also more user friendly, because it is easy to use, and more comfortable to wear. Arduino UNO based sensor, instead, has higher variability in the data, maybe due to the presence of movement artefacts. In fact, the fingers are more prone to involuntary imperceptible movements. In order to obtain a significant signal, a response high enough to overcome the intrinsic variability linked to this sensor should be evoked in the subject performing the tests. Moreover, its use as a wearable device is not realistic without making substantial changes in the different device components.

Another possible future development of this study to consider, is the narrowing of the age range to which subjects belong, since it was seen that in the case of Subject 3, the oldest in age, it was difficult to make consistent comparisons. A subject-dependent classification approach is also to be considered [8]. Giving in advance some information about the subject to the system and involving a learning phase for each subject prior to the classification, could lead to a more user-specific activity recognition.

# Chapter 7

# Future developments

In this study, 16 different features for physical stress induced GSR recognition have been computed and analysed, but the number of involved subjects was not high enough to bring the study to general statements. The repetition of the experiment, opened to a higher number of recruited subjects, could be helpful to obtain more consistent and reliable results. Repeating the test in contexts different from the physical activity, could be interesting to evaluate if the selected features are sensitive to changes in arousal elicited by other kind of stimuli, or if it may be necessary to focus on different features that better capture different EDA signal patterns, useful for the physical effort intensity classification. For the frequency domain analysis, a possible improvement could be achieved by the computation of the features on the signal portion confined in the frequency range [0-0.5] Hz, in order to limit the results to a region with maximum information content. Finally, a greater number of subjects could represent an opportunity to build a homogeneous training set for the training of a subject-dependent classification model, capable to consider individual differences. This may reduce the risk of misclassification and, considering the feature selection, to reduce the computational cost. These are basic requirements for the development of real time activity recognition algorithms to be embedded in wearable devices.

# References


[1] Benedek, Mathias, and Christian Kaernbach. "A continuous measure of phasic electrodermal activity." *Journal of neuroscience methods* 190.1 (2010): 80-91.

[2] Hernando-Gallego, Francisco, David Luengo, and Antonio Artés-Rodríguez. "Feature extraction of galvanic skin responses by nonnegative sparse deconvolution." *IEEE journal of biomedical and health informatics* 22.5 (2017): 1385-1394.

[3] Can, Yekta Said, et al. "Continuous stress detection using wearable sensors in real life: Algorithmic programming contest case study." *Sensors* 19.8 (2019): 1849.

[4] Schoenberg, Poppy LA, and Anthony S. David. "Biofeedback for psychiatric disorders: a systematic review." *Applied psychophysiology and biofeedback* 39.2 (2014): 109-135.

[5] https://www.zyto.com/what-can-electrodermal-activity-measurements-tell-you

[6] Caruelle, Delphine, et al. "The use of electrodermal activity (EDA) measurement to understand consumer emotions–A literature review and a call for action." *Journal of Business Research* 104 (2019): 146-160.

[7] https://imotions.com/blog/galvanic-skin-response/

[8] Shukla, Jainendra, et al. "Feature Extraction and Selection for Emotion Recognition from Electrodermal Activity." *IEEE Transactions on Affective Computing* (2019).

[9] https://www.sweathelp.org/about-hyperhidrosis/physiology-of-normal-sweating.html

[10] https://opentextbc.ca/anatomyandphysiology/chapter/5-1-layers-of-the-skin/

[11] Benedek, Mathias, and Christian Kaernbach. "Decomposition of skin conductance data by means of nonnegative deconvolution." *Psychophysiology* 47.4 (2010): 647-658.

[12] Boucsein, Wolfram. *Electrodermal activity*. Springer Science & Business Media, 2012.

[13] Alexander, David M., et al. "Separating individual skin conductance responses in a short interstimulus-interval paradigm." *Journal of neuroscience methods* 146.1 (2005): 116-123.

[14] Fowles, Don C., et al. "Publication recommendations for electrodermal measurements." *Psychophysiology* 18.3 (1981): 232-239.

[15] https://mindfield-esense.com/esense-skin-response-it/

[16] Dawson, Michael E., Anne M. Schell, and Diane L. Filion. "The electrodermal system." (2017).

[17] Posada-Quintero, Hugo F., et al. "Time-varying analysis of electrodermal activity during exercise." *PloS one* 13.6 (2018).

[18] Chowdhury, Alok Kumar, et al. "Prediction of relative physical activity intensity using multimodal sensing of physiological data." *Sensors* 19.20 (2019): 4509.

[19] Girardi, Daniela, Filippo Lanubile, and Nicole Novielli. "Emotion detection using noninvasive low cost sensors." *2017 Seventh International Conference on Affective Computing and Intelligent Interaction (ACII)*. IEEE, 2017.

[20] https://www.empatica.com/en-eu/research/e4/

[21] https://www.mayoclinic.org/healthy-lifestyle/fitness/in-depth/exercise-intensity/art-20046887

[22] Al Machot, Fadi, et al. "A deep-learning model for subject-independent human emotion recognition using electrodermal activity sensors." *Sensors* 19.7 (2019): 1659.

[23] van Dooren, Marieke, and Joris H. Janssen. "Emotional sweating across the body: Comparing 16 different skin conductance measurement locations." *Physiology & behavior* 106.2 (2012): 298-304.

[24] Poh, Ming-Zher, Nicholas C. Swenson, and Rosalind W. Picard. "A wearable sensor for unobtrusive, long-term assessment of electrodermal activity." *IEEE transactions on Biomedical engineering* 57.5 (2010): 1243-1252.

[25] Hui, Terence KL, and R. Simon Sherratt. "Coverage of emotion recognition for common wearable biosensors." *Biosensors* 8.2 (2018): 30.

[26] Vieluf, Solveig, et al. "Exercise-induced changes of multimodal interactions within the autonomic nervous network." *Frontiers in physiology* 10 (2019): 240.

[27] de Hospitales Vithas, Servicio de Neurorrehabilitación. "Reliability of the Empatica E4 wristband to measure electrodermal activity to emotional stimuli."

[28] Ji, Xiaoyong, et al. "Research on the Electrodermal Activity during Walking and Running." *2019 4th International Conference on Control and Robotics Engineering (ICCRE)*. IEEE, 2019.

[29] Menghini, Luca, et al. "Stressing the accuracy: Wrist-worn wearable sensor validation over different conditions." Psychophysiology 56.11 (2019): e13441.

[30] Ollander, Simon, et al. "A comparison of wearable and stationary sensors for stress detection." *2016 IEEE International Conference on Systems, Man, and Cybernetics (SMC)*. IEEE, 2016.

[31] Shu, Lin, et al. "A review of emotion recognition using physiological signals." *Sensors* 18.7 (2018): 2074.